# Oct4 mediated inhibition of Lsd1 activity promotes the active and primed state of pluripotency enhancers

Lama AlAbdi[1], Debapriya Saha[1], Ming He[1], Mohd Saleem Dar[1], Sagar M. Utturkar[2], Putu Ayu Sudyanti[3], Stephen McCune[1], Brice, H. Spears[1], James A. Breedlove[1], Nadia A. Lanman[2,4], Humaira Gowher[1,2*]

[1]Department of Biochemistry; [2]Purdue University Center for Cancer Research; [3]Department of Statistics; [4]Department of Comparative Pathobiology; Purdue University; West Lafayette, Indiana 47907 USA

*Correspondence: hgowher@purdue.edu

**Running title:** Loss of Lsd1 regulation in carcinoma cells

## Summary

Enhancer reactivation and pluripotency gene (PpG) expression were recently shown to induce stemness and enhance tumorigenicity in cancer stem cells. Silencing of PpG enhancers during embryonic stem cell differentiation involves changes in chromatin state, facilitated by the activity of Lsd1/Mi2-NuRD-Dnmt3a complex. In this study, we observed a widespread retention of H3K4me1 at PpG enhancers and partial repression of PpGs in F9 embryonal carcinoma cells (ECCs) post differentiation. Absence of H3K4me1 demethylation could not be rescued by Lsd1 overexpression. Based on the observation that H3K4me1 demethylation is accompanied by strong Oct4 repression in P19 ECCs, we tested if Lsd1-Oct4 interaction modulates Lsd1 activity. Our data show a dose dependent inhibition of Lsd1 by Oct4 *in vitro* and retention of H3K4me1 at PpG enhancers post differentiation in Oct4 overexpressing P19 ECCs. These data reinforce that Lsd1-Oct4 interaction in cancer stem cells could establish a *primed* enhancer state, which is susceptible to reactivation.

**Keywords:** Pluripotency, enhancers, Dnmt3a, DNA methylation, embryonal carcinoma cells, Lsd1, histone demethylation, Oct4, cancer stem cells, enhancer priming.

## Introduction

Cell type specific gene expression is regulated by chromatin conformation which facilitates the interaction of distally placed enhancer elements with the specific gene promoter (Banerji et al., 1981, Bulger and Groudine, 2011, Ong and Corces, 2011, Plank and Dean, 2014). Enhancers house majority of transcription factor binding sites and amplify basal transcription thus playing a critical role in signal dependent transcriptional responses (summarized in (Heinz et al., 2015)). Epigenome profiling combined with the transcriptional activity in various cell types led to identification of potential enhancers, which are annotated as silent, primed, and active based on their epigenetic features. These epigenetic features include histone modifications, DNA

methylation, and enhancer-associated RNA (eRNA) (Ernst and Kellis, 2010, Ernst et al., 2011, Calo and Wysocka, 2013). Whereas histone H3K4me1 (monomethylation) and H3K4me2 (dimethylation) is present at both active and primed enhancers, active enhancers invariantly are marked by histone H3K27Ac (acetylation) and are transcribed to produce short read eRNA (Heintzman et al., 2007, Heinz et al., 2010, Rada-Iglesias et al., 2011, Creyghton et al., 2010, Zentner et al., 2011).

During embryonic stem cell (ESC) differentiation, pluripotency gene (PpG) specific enhancers are silenced via changes in histone modifications and gain of DNA methylation (Whyte et al., 2012, Mendenhall et al., 2013, Petell et al., 2016). In response to the differentiation signal, the coactivator complex (Oct4, Sox2, Nanog and Mediator complex) dissociates from the enhancer followed by the activation of pre-bound Lsd1-Mi2/NuRD enzymes. The histone demethylase, Lsd1, demethylates H3K4me1, and HDAC in NuRD complex deacetylates the H3K27Ac (Whyte et al., 2012). Our previous studies have shown that the histone demethylation event is critical for the activation of DNA methyltransferase Dnmt3a, which interacts with the demethylated histone H3 tails through its chromatin-interacting ADD (ATRX-Dnmt3a-Dnmt3L) domain allowing site-specific methylation at pluripotency gene enhancers (PpGe) (Petell et al., 2016). These studies also suggest that an aberrant inhibition of Lsd1 activity could cause a failure to gain DNA methylation leading to incomplete repression of PpGs.

Several studies have reported on potential mechanisms that control site specific targeting and catalytic activity of Lsd1. It was shown that whereas the interaction with CoREST activates the enzyme, BHC80 inhibits Lsd1 demethylation activity (Shi et al., 2005). The substrate specificity of Lsd1 is regulated by its interaction with androgen receptor and estrogen related receptor α, or by alternative splicing which add four or eight amino acids to the Lsd1 enzyme (Carnesecchi et al., 2017, Metzger et al., 2005, Laurent et al., 2015, Zibetti et al., 2010, Wang et al., 2015a). Lsd1 is targeted to various genomic regions through its interaction with SNAG domain containing TFs,

such as Snail and GFI1B (McClellan et al., 2019, Vinyard et al., 2019). SNAG domain binds to the active site of Lsd1 by mimicking histone H3 tail and could potentially inhibit its activity (Baron et al., 2011). Interaction of p53 C' terminal domain with Lsd1 active site inhibits its enzymatic activity (Speranzini et al., 2017). Lsd1 was also shown to be present in the Oct4 interaction network, and therefore could be targeted to Oct4 bound regulatory elements which largely control pluripotency and stemness (Pardo et al., 2010, van den Berg et al., 2010).

Studies by the Cancer Genome Anatomy Project (CGAP) show that one out of three cancers express PpGs suggesting their role in dysregulated proliferation during tumorigenesis (Zhang et al., 2013, Liu et al., 2013). Further, expression of PpGs, *Oct4*, *Sox2* and *Nanog*, potentiates self-renewal of putative cancer stem cells (CSCs) (Ben-Porath et al., 2008, Feske, 2007, Linn et al., 2010, Peng et al., 2010, Kumar et al., 2012, Wang et al., 2013, Mak et al., 2012, Wen et al., 2010, Jeter et al., 2011). CSCs proliferate as well as differentiate to give rise to cancer cells of various lineages (Iglesias et al., 2017). However, in order to retain the ability to proliferate, many cancer cells maintain expression of PpGs (Gwak et al., 2017, Yang et al., 2018). This has led to the development of terminal differentiation therapy, which aims to limit the proliferating cancer cell population (de The, 2018). Embryonal Carcinoma cells (ECCs) have been used as model cell line to study CSCs. ECCs were derived from developing mouse embryos at E6-7.5 and share regulatory characteristics with ESCs including their ability to differentiate into various somatic lineages (Alonso et al., 1991, Han et al., 2017, Andrews et al., 2005, Zhu et al., 2013). To understand the mechanism by which cancer cells retain PpG expression, we investigated the mechanism of enhancer-mediated regulation of PpG expression in ECCs. Our data showed in differentiating F9 ECCs, that the PpGs are partially repressed. This was concomitant with H3K27 deacetylation but an absence of Lsd1- mediated H3K4me1 demethylation at PpGe. Presence of H3K4me1 prevented Dnmt3a from methylating the DNA at these sites potentially abrogating PpGe silencing. Drug-mediated inhibition as well as overexpression of Lsd1 had little or no effect

on enhancer silencing and PpG repression confirming a loss of Lsd1 dependence. Given that Oct4 was expressed at substantial levels in F9 ECCs post differentiation, we investigated the effect of Lsd1-Oct4 interaction on Lsd1 catalytic activity. Using *in vitro* histone demethylation assays, we discovered that Lsd1-Oct4 interaction inhibits the Lsd1 activity potentially causing retention of H3K4me1 at PpGe in F9 ECCs. We tested this prediction in P19 ECCs in which we observed H3K4me1 demethylation at PpGe accompanied by loss of Oct4 expression post differentiation. Overexpression of Oct4 in differentiating P19 ECCs led to retention of H3K4me1 at PpGe confirming the role of Oct4-mediated Lsd1 inhibition at these sites. Taken together our data show that inhibition of Lsd1 activity and Dnmt3a leads to the establishment of a "primed" enhancer state, which is open for coactivator binding and prone to reactivation. We speculate that aberrant expression of Oct4 in CSCs facilitates the establishment of "primed" enhancers, reactivation of which support tumorigenicity.

## Results:

### PpGs are partially repressed in differentiating F9 ECCs

ECCs share many characteristics with ESCs including mechanisms governing regulation of gene expression and differentiation (Alonso et al., 1991). Based on the observation that aberrant PpG expression is commonly found in cancers (Zhang et al., 2013, Liu et al., 2013), we compared the magnitude of PpG repression in F9 ECCs with that in ESCs pre- and post-differentiation. F9 ECCs and ESCs were induced to differentiate with retinoic acid (RA) and expression of eight PpGs at 4 and 8 days (D4 and D8) post induction was measured by RT-qPCR. The data show that in differentiating F9 ECCs, several PpGs were incompletely repressed, of which the pioneer factors Oct4 and Nanog showed only 50% loss of expression at D8 post differentiation. Comparatively in ESCs, the expression of most PpGs was reduced by more than 80% at D4 post differentiation (Figures 1A and 1B). The expression of *Sox2* and *Trim28* was maintained post differentiation as an anticipated response to RA signaling guiding

ESCs towards neural lineage. A substantial increase in the expression of *Lefty1* and *Lefty2* genes in F9 ECCs suggests potential activation of germ cell and testis development program (Zhu et al., 2013). Continued expression of PpGs in F9 ECCs was also evident by positive alkaline phosphatase staining and SSEA-1 immunofluorescence in differentiating F9 ECCs that is completely lost in ESCs post differentiation (Figures 1C and 1D). We asked if failure to exit pluripotency in F9 ECCs was caused by an inability to activate lineage-specific genes. Our data showed 10-50 fold increase in expression of the lineage specific genes *Gata4, FoxA2, Olig2, Gata6, Cxcr4 and Fgf5* (Figure 1E), endorsing a standard response to signal of differentiation. Given that previous studies in ESCs have established a critical role of enhancer silencing in complete PpG repression, we next investigated if PpGe were fully decommissioned in F9 ECCs post differentiation**.

**DNA methylation is not established at PpGe during F9 ECC differentiation**

We have previously reported that in differentiating ESCs, PpGe decommissioning involves gain of DNA methylation, which is required for complete PpG repression. (Petell et al., 2016). We used bisulfite sequencing (Bis-Seq) to compare DNA methylation changes at a subset of PpGe in F9 ECCs to that in ESCs post differentiation. Whereas DNA methylation was significantly gained in ESCs within 4 days post differentiation, the PpGe remained hypomethylated in F9 ECCs at 4 and 6 days post differentiation (Figures 2A, 2B, and S1A). A similar hypomethylated state persisted at PpG promoters in F9 ECCs except the highly methylated *Lefty2* promoter, where DNA methylation was partially lost post differentiation (Figure S1B). This is consistent with the observed partial repression of most PpGs and an induction of *Lefty2* expression in these cells (Figure 1A).

We confirmed that absence of DNA methylation at PpGe was not due to the low expression of Dnmt3a in F9 ECCs post differentiation (Figures S1C and S1D). Based on the previous observations in cancers that overexpression of DNA methyltransferases leads to DNA

hypermethylation (Yu et al., 2015, Gao et al., 2015, Ma et al., 2018, Jones et al., 2016, Schübeler, 2015), we tested if overexpression of Dnmt3a could rescue DNA methylation at PpGe. F9 ECCs were transfected with Myc-Dnmt3a and differentiated at 24 hrs post transfection to ensure expression of recombinant Dnmt3a during differentiation (Figure S1E). However, we observed no gain in DNA methylation at PpGe and no additional decrease in the expression of PpGs when compared to untransfected cells at D8 post differentiation (Figures 2C and 2D).

We next assayed DNA methylation genome-wide using MethylRAD sequencing to analyze changes at all PpGe in F9 ECCs pre- and post-differentiation (Wang et al., 2015b). Similar to methylation dependent restriction assays, this method uses FsPEI enzyme, which cuts DNA bidirectionally from mC to create 31-32 bp fragment (Cohen-Karni et al., 2011, Zheng et al., 2010). The restriction fragments were isolated for library preparation and high throughput sequencing. Using this method, we captured DNA methylation at 1,370,254 cytosines genome-wide, requiring a minimum read support of 5 reads. The reads were distributed among all chromosomes representing all annotated genomic elements (Figure S2A). DNA methylation levels at enhancers (low-intermediate-high) were calculated based on highest (75th percentile) and lowest (25th percentile) number of reads at all annotated enhancers in the genome, which were obtained from the EnhancerAtlas 2.0. We filtered the data to focus our analysis on DNA methylation changes at 3840 PpGe previously annotated in ESCs as Lsd1 bound regions (Whyte et al., 2012). Our method identified 1,865 PpGe in F9 ECCs. Compared to methylation levels at all other known enhancers, the PpGe cluster in low/intermediate methylation group (Figure S2B). The difference in methylation for each PpGe region was computed by subtracting the DNA methylation level in D4 differentiated from that in undifferentiated F9 ECCs. The data show around 1488 (82%) regions fail to gain DNA methylation post differentiation of F9 ECCs (no change in DNA methylation; NCDM PpGe) (Figure 2E). To determine the function of genes

associated with NCDM PpGe, we performed *Ingenuity* pathway analysis (IPA) (www.qiagen.com/ingenuity), which showed a significant enrichment of Oct4 and Nanog regulated mammalian embryonic stem cell and molecular mechanisms of cancer pathways (Figure 2F).

Given that DNA methylation by Dnmt3a at PpGe requires H3K27 deacetylation and H3K4 demethylation by Lsd1/Mi2NurD complex (Whyte et al., 2012), we anticipate a potential impediment in this process causing a widespread failure to acquire DNA methylation at PpGe.

**A "primed" PpGe state is established during F9 ECC differentiation**

We asked if the chromatin state at PpGe in F9 ECCs is impermissible to DNA methylation. Using chromatin immunoprecipitation followed by qPCR (ChIP-qPCR) we examined histone H3K27 deacetylation and our data showed a decrease in H3K27Ac at PpGe in F9 ECCs post differentiation. This suggests that similar to ESCs, PpGe are active in undifferentiated F9 ECCs and initiate the decommissioning process post differentiation (Figures S3A and 3A). Furthermore, deacetylation at *Lefty1* and *Lefty2* enhancers suggests enhancer-switching involving the potential use of germline-specific enhancers post differentiation leading to an observed increase in *Lefty1* and *Lefty2* expression (Figure 1A). Numerous studies have proposed that deacetylation of H3K27Ac followed by H3K27 methylation by PRC2 enzyme complex establishes a silenced state (Lindroth et al., 2008, Barski et al., 2007, Wang et al., 2008). Our data showed no increase of H3K27me3 at the PpGe in both ESCs as well as F9 ECCs post differentiation suggesting that PRC2 activity is unessential for the PpGe silencing (Figures S3B and S3C).

We next monitored H3K4me1 demethylation activity of Lsd1 at PpGe during F9 ECC differentiation. Surprisingly, we observed a retention or an increase in H3K4me1 at five out of seven tested PpGe post differentiation (Figure 3B) suggesting a potential disruption of Lsd1

activity. We verified similar expression levels of Lsd1 in F9 ECCs compared to ESCs (Figures S1C and S1D). To examine if Lsd1 interacts with Mi2/NuRD complex in F9 ECCs, we performed co-immunoprecipitation (Co-IP) experiments using whole cell extracts. Antibodies against Lsd1 and HDAC1 were used for reciprocal Co-IP. The data show the presence of Chd4, HDAC1 and Lsd1 and no significant difference in protein complexes between ESCs and F9 ECCs (Figure S3D). To test its recruitment to PpGe, ChIP-qPCR showed similar enrichment of Lsd1 in F9 ECCs and ESCs at four tested enhancers (Figure 3C).These data suggest that retention of H3K4me1 at PpGe is caused by lack of Lsd1 activity in F9 ECCs post differentiation.

To confirm the above conclusion we next tested the effect of Lsd1 overexpression or inhibition on PpGe silencing and PpG repression in differentiating F9 ECCs. F9 ECCs were transfected with FLAG-Lsd1 overexpressing plasmid and differentiated at 24 hrs post transfection (Figure S4A). We observed no change in H3K4me1 at PpGs post differentiation, rather a small increase at some enhancers, indicating an inhibitory mechanism which affects Lsd1 irrespective of its origin (Figure 3D). An increase in H3K4me1 post differentiation could be due to partial activity of Lsd1 by which it demethylates H3K4me2 to H3K4me1 at these sites. Additionally, Lsd1 overexpression had no effect on PpG repression or DNA methylation at PpGe post differentiation (Figures S4B and S4C).

Previous studies in ESCs have shown that treatment with Lsd1 inhibitors pargyline and TCP (tranylcypromine) at the onset of differentiation results in H3K4me1 retention at PpGe and incomplete repression of PpGs (Whyte et al., 2012). F9 ECCs were treated with pargyline and TCP 6 hrs prior to induction of differentiation. In contrast to 70-80% cell death caused by Lsd1 inhibitor in ESCs, F9 ECCs remained largely viable upon treatment (Figure S4D). Expression analysis of PpGs showed a slight relief of PpG repression in treated cells, suggesting a partial Lsd1 activity at PpGe (Figure S4E). Interestingly, pargyline treatment affected the H3K4me1 enrichment gained post differentiation in untreated cells (WT and Lsd1 overexpressing) confirming the partial activity of Lsd1 at these sites (Figure 3E). To test if Lsd1 activity

contributed to the generation of H3K4me1 in undifferentiated state, we transiently overexpressed Lsd1 in F9 ECCs and allowed cells to grow for 72 hrs. ChIP-qPCR analysis showed no increase in H3K4me1 levels in Lsd1 overexpressing cells (Figure S4F). This suggests that similar to ESCs the deposition of H3K4me1 in the undifferentiated F9 ECCs is largely accomplished by MLL3/4 histone methyltransferases and Lsd1 activity at these sites is initiated only in response to a differentiation signal (Mak et al., 2012, Yegnasubramanian et al., 2011).

Taken together these observations propose that the restricted activity of Lsd1 at PpGe leads to retention of H3K4me1 post differentiation. Moreover, following the deacetylation of H3K27, absence of DNA methylation and presence of H3K4me1 yields these enhancers in a “primed” state, prone to reactivation in presence of a coactivator.

**High throughput analysis of changes in H3K4me1 at PpGe**

To identify and enumerate PpGe with aberrant retention of H3K4me1 post differentiation, we performed ChIP-Seq analysis of H3K4me1 genome-wide in undifferentiated and D4 differentiated F9 ECCs. Peak calling was performed using Epic2 for each input-ChIP pair and the list was filtered to calculate the number of peaks with cut off (FDR<=0.05 and Log2FC>=2) (Figure S5A). We analyzed the distribution of H3K4me1 peaks at the regulatory elements across the genome (Figure S5B). For further analysis, we identified 1425 H3K4me1 peaks found within 1kb of PpGe previously annotated in ESCs (Whyte et al., 2012). The difference in peak enrichment (i.e. log2FoldChange) between differentiated and undifferentiated was calculated to score for change in H3K4me1 post differentiation. The data showed no change, increase, and decrease in 733, 510, and 182 PpGe respectively. Therefore 87% of PpGe showed no significant decrease in H3K4me1 (no decrease in histone methylation; NDHM PpGe) (Figure 4A). We next computed correlation between the three PpGe sub-groups and the 1792 PpGe that undergo H3K4me1 demethylation in differentiating ESCs (Whyte et al., 2012). The

data showed that a significant fraction of NDHM PpGe, which exhibit an increase (74%) or no change (69%) in H3K4me1 in F9 ECCs overlap with PpGe that are H3K4me1 demethylated in ESCs (Figures 4B, 4C, and S5C). These observations strongly support our previous conclusion that in F9 ECCs, Lsd1 activity is inhibited leading to retention of H3K4me1 at PpGe. IPA of NDHM PpGe –associated genes showed highest enrichment for Oct4-regulated and stem cell pathways. Comparatively, genes associated with PpGe, which undergo H3K4me1 demethylation show enrichment for signaling pathways (Figures 4D and S5D). A correlation between NCDM and NCHM PpGe, showed that 65% of NDHM PpGe fail to acquire DNA methylation underpinning the role of histone demethylation in the regulation of DNA methylation at PpGe (Figure 4E) (Petell et al., 2016).

**Lsd1 activity at PpGe is inhibited by its interaction with Oct4**

Next, we sought to determine the mechanism that inhibits Lsd1 activity. Due to its continued expression in F9 ECCs post differentiation, we assumed that Oct4 remains associated with PpGe and prevents demethylation of H3K4me1. We tested this hypothesis in P19 ECCs in which Oct4 expression was reported to be strongly repressed post differentiation (Li et al., 2007). After confirming a 90% reduction in Oct4 expression (Figure 5A), we probed H3K4me1 demethylation at PpGe during P19 ECC differentiation. Indeed, our data show decreased enrichment of H3K4me1 at PpGe 4 days post differentiation (Figure 5B). Similar to ESCs, we also observed a massive cell death when P19 ECCs were exposed to Lsd1 inhibitor during differentiation (Figure S6A). The change in the chromatin state was accompanied by 40% gain of DNA methylation at these sites (Figure 5C).

This observation together with the IPA showing enrichment of Oct4-regulated genes in NCHM and NCDM enhancers, suggested that Oct4 may regulate the demethylase activity of Lsd1 at PpGe. Co-precipitation experiments using recombinant proteins, GST-Lsd1 and Oct4, confirmed a direct interaction between Oct4 and Lsd1 (Figure 6A). This is concurrent with previous reports

which suggested that Oct4 interacts with Lsd1 and the Mi2/NuRD complex in ESCs (van den Berg et al., 2010, Pardo et al., 2010). To test the effect of Oct4 interaction on Lsd1 catalytic activity, we performed Lsd1 demethylation assays using H3K4me2 peptide as a substrate. Our data showed that in the presence of Oct4, Lsd1 activity was reduced to by 60-70% in a dose dependent manner. This reduction in activity was not observed in the presence of recombinant Dnmt3a protein (Figures 6B and 6C). We also performed Lsd1 demethylation assays using purified histones as a substrate and detected H3K4me2 demethylation on a Western blot. The data clearly shows reduced H3K4me2 signal in presence of Lsd1 which was rescued in presence of 0.1mM TCP. An accumulation of H3K4me2 signal with an increase in Oct4 concentration in reaction mix clearly show an enhanced inhibition of Lsd1 activity by Oct4 (Figure 6D). These data suggest that in F9 ECCs, due to its continued expression post differentiation, Oct4 remains bound at PpGe and inhibits Lsd1. We tested this prediction directly by stably expressing recombinant Oct4 in P19 ECCs (Figure S6B). Following differentiation of Oct4-expressing P19 cells, examination of H3K4me1 showed retention of this mark at PpGe indicating the inhibition of Lsd1 by recombinant Oct4 (Figure 6E).This was accompanied by a derepression of several PpGs and reduced gain in DNA methylation at their respective enhancers (Figures 6F and 6G).

Taken together we propose the following model that explains the regulation of Lsd1 activity at PpGe. At the active PpGe, Lsd1 activity is inhibited by its interaction with bound Oct4. Post differentiation, this inhibition is relieved by dissociation of Oct4 from its binding sites. However, in cancer cells where Oct4 expression is maintained, Lsd1 is held in its inhibited state leading to incomplete demethylation. Retention of H3K4me1 in turn blocks the activation of Dnmt3a from its autoinhibited state resulting in absence of DNA methylation at PpGe. The absence of DNA methylation and presence of H3K4me1 yields these enhancers in a “primed” state, prone to activation in presence of a coactivator (Figure 7). Based on previous reports that Oct4 as well

as Lsd1 are aberrantly expressed in several cancers (Kim et al., 2015, Wang et al., 2010, Schoenhals et al., 2009, Wang et al., 2009, Kashyap et al., 2013, Lv et al., 2012, Hosseini and Minucci, 2017), Oct4-Lsd1 interaction could misdirect Lsd1 activity leading to aberrant gene expression.

## Discussion

The preservation of epigenetic state of enhancers in various cell types indicates that aberrant changes could promote tumorigenesis which is supported by recent studies revealing a crucial role for enhancer-mediated activation of oncogenes (Hnisz et al., 2015, Mansour et al., 2014, Chapuy et al., 2013, Groschel et al., 2014, Loven et al., 2013).Changes in H3K4me1 levels and DNA accessibility at various enhancers have been reported in many cancers (Akhtar-Zaidi et al., 2012). Some studies also propose the role of change in enhancer state in therapy resistance in cancer cells. These studies showed loss or gain of H3K4me1/2 at the enhancers was reported in resistant breast cancer cells and loss of H3K27 acetylation at enhancers in T cell acute lymphoblastic leukemia (T-ALL) (Magnani et al., 2013, Knoechel et al., 2014). In addition, DNA hypermethylation concomitant with overexpression of DNA methyltransferases is a hallmark of many cancers (Jones et al., 2016, Schübeler, 2015). Changes in DNA methylation at enhancers have been shown in breast, lung, prostate and cervical cancers (Taberlay et al., 2014, Aran and Hellman, 2013, Aran et al., 2013, Yegnasubramanian et al., 2011). These studies suggest that chromatin state of enhancers can be used as a diagnostic to predict aberrant expression of tissue specific genes in cancer. Our data showing a coherent response of PpGe to signals of differentiation in ESCs supports this prediction. During ESC differentiation, all tested PpGe undergo histone deacetylation and gain of DNA methylation, irrespective of the transcriptional status of the associated gene. This is exemplified by H3K27Ac deacetylation and gain of DNA methylation at *Sox2* and *Trim28* enhancers despite the maintained expression of these genes.

Our study here reveals a mechanism by which developmental enhancers could acquire aberrant histone modification and DNA methylation states that affect gene expression. We show in F9 ECCs, that compromised activity of histone demethylase, Lsd1, causes retention of H3K4me1 and absence of DNA methylation at the PpGe, leading to a primed state of enhancers. Unlike the silenced state, the “primed” enhancer state grants accessibility for coactivator binding which renders cells highly vulnerable to small increase in the expression of oncogenic coactivators or master transcription factors (Zaret and Carroll, 2011, Calo and Wysocka, 2013).

We uniquely discovered that Lsd1 activity is inhibited by its interaction with the pioneer transcription factor Oct4, which is expressed at a substantial level in F9 ECCs post differentiation. Recently similar observation was reported from flow cytometric analysis showing that compared to ESCs, a significantly higher number of F9 ECCs have persistent *Oct4* expression post differentiation (Gordeeva and Khaydukov, 2017). Aberrant expression of *Oct4*, *Sox2*, and *Nanog* is associated with tumor transformation, metastasis, and drug resistance (Sampieri and Fodde, 2012, Ben-Porath et al., 2008). We speculate that during differentiation of cancer stem cells, inhibition of Lsd1 by Oct4 leads to PpGe priming/reactivation which enhances PpG expression. Our studies further highlight the versatility of Lsd1 binding and activity which can be fine-tuned by its interaction with numerous factors allowing the enzyme to function in various cellular processes including differentiation and disease.

## Acknowledgements

We are thankful to Gowher lab members for discussions. This work was supported by NIHR01GM118654-01 and graduate fellowship for LA from King Saud University. The authors gratefully acknowledge the Walter Cancer Foundation, DNA Sequencing Facility, and support from the Purdue University Center for Cancer Research, P30CA023168. We thank Dr. Phillip SanMiguel from Genomic Core, Purdue for analysis of Bis-Seq data and Dr. Taiping Chen for providing FLAG-Lsd1 and Myc-Dnmt3a2 expression plasmids.

## Authors Contributions

L.A., S.M., B.H., J.B., M.H., D.S., and M.S.D performed the experiments. N.A., S.U., and P.A.S. analyzed the genome-wide data. L.A. and H.G. wrote the manuscript

## Declaration of Interests

None declared.

## Figure Legends

**Figure 1. Pluripotency genes are partially repressed in F9 embryonal carcinoma cells.**

UD: undifferentiated; D4, D8: Days post induction of differentiation; ESCs: embryonic stem cells and F9 ECCs: F9 embryonal carcinoma cells, PpGs: pluripotency genes.

(A, B, and E) Gene expression analysis by RT-qPCR of PpGs in (A) F9 ECCs, (B) ESCs (E) lineage specific genes in F9 ECCs. The $C_t$ values for each gene were normalized to *Gapdh* and expression is shown relative to that in undifferentiated cells (dotted line). In F9 ECCs, the lineage specific genes show 40-60 fold induction of gene expression (E) whereas the expression of PpGs is on average reduced to about 50% post differentiation (B). Average and SEM of two biological replicates are shown for each gene.

(C) Alkaline phosphatase staining and (D) SSEA-1 immunofluorescence of ESCs and F9 ECCs pre- and post-differentiation. Positive signal indicates pluripotency that is lost post differentiation in ESCs. The scale bar is a 100μm.

**Figure 2. Pluripotency gene enhancers do not gain DNA methylation in differentiating F9 embryonal carcinoma cells.**

UD: undifferentiated; D4, D8: Days post induction of differentiation; D8 UT: untransfected F9 ECCs differentiated for 8 days; D8+Myc-Dnmt3a: F9 ECCs overexpressing Myc-Dnmt3a and differentiated for 8 days; ESCs: embryonic stem cells and F9 ECCs: F9 embryonal carcinoma cells; PpGe: pluripotency gene enhancers.

(A, B, and C) DNA methylation analysis using Bis-Seq. Genomic DNA was treated with bisulfite and PpGe regions were amplified by PCR. The amplicons were sequenced on a high throughput sequencing platform (Wide-Seq) and the data were analyzed using Bismark software. DNA methylation of PpGe in (A) ESCs (B) F9 ECCs pre- and post-differentiation. Less

than 10% DNA methylation was recorded in F9 ECCs whereas H19 imprinted region, used as a control, showed DNA methylation at 80%. At the same regions, DNA methylation increased up to 30% in ESCs. See also Figure S1A.

(C) DNA methylation of PpGe in F9 ECCs overexpressing Myc-Dnmt3a. (D) Gene expression analysis by RT-qPCR PpGs in F9 ECCs overexpressing Myc-Dnmt3a pre- and post-differentiation. (C, D) show no significant increase in DNA methylation or gene repression 8 days post differentiation The $C_t$ values for each gene were normalized to *Gapdh* and expression is shown relative to that in undifferentiated cells (dotted line). Data for A, B, C and D are the average and SEM of two biological replicates.

(E) Genome-wide DNA methylation analysis by MethylRAD sequencing. Genomic DNA was digested with the restriction enzyme FspEI that cuts methylated DNA into 31-32 bp fragments. The fragments were sequenced and mapped on mm10 mouse genome. The number of reads per region were used as a measure for extent of DNA methylation and compared between undifferentiated and D4 differentiated F9 ECCs. The waterfall plot shows DNA methylation changes at PpGe computed by subtracting normalized counts in D4 samples from normalized counts in undifferentiated samples. Upper and lower quartiles were used in thresholding regions as gaining or losing methylation. The pie chart shows fractions of PpGe with increase, decrease or no change in DNA methylation (NCDM). See also Figure S2B.

(F) Top ten statistically significant enriched canonical pathways amongst the genes associated with the NCDM enhancers, which showed no change. The x-axis shows the $\log_{10}$(adjusted p-value), with the p-value adjusted for multiple testing using the Benjamini-Hochberg method.

**Figure 3. Changes in chromatin modifications establish a "primed" state at pluripotency gene enhancers in F9 embryonal carcinoma cells.**

UD: undifferentiated; D4: Days post induction of differentiation; D4+FLAG-Lsd1: F9 ECCs overexpressing FLAG-Lsd1 and differentiated for 4 days; Prg: Pargyline; ESCs: embryonic stem cells and F9 ECCs: F9 embryonal carcinoma cells; PpGe: pluripotency gene enhancers.

(A-E) Chromatin immunoprecipitation (ChIP)-qPCR assays showing percent enrichment over input. Histone modifications at PpGe (A) H3K27Ac and (B) H3K4me1 in F9 ECCs pre- and D4 post differentiation. Whereas deacetylation of PpGe is observed as a decrease in H3K27Ac signal, histone H3K4me1 is retained post differentiation.

(C) Similar Lsd1 occupancy in undifferentiated ESCs and F9 ECCs.

(D) Enrichment of H3K4me1 in F9 ECCs expressing recombinant FLAG-Lsd1 compared to untransfected cells at D4 post differentiation. There is a slight increase in H3K4me1 at some PpGe.

(E) Fold change in enrichment of H3K4me1 at PpGe in pargyline treated and untreated, WT and FLAG-Lsd1 overexpressing F9 ECCs, at D4 post differentiation. Fold change is represented as relative to enrichments in the undifferentiated state (dotted line).

**Figure 4. Retention of H3K4me1 at most pluripotency gene enhancers in F9 ECCs post differentiation.**

ESCs: embryonic stem cells and F9 ECCs: F9 embryonal carcinoma cells; PpGe: pluripotency gene enhancers; D4: Days post induction of differentiation

Genome-wide H3K4me1 levels in F9 ECCs pre- and post-differentiation were measured by ChIP-Seq. Peak calling was performed using Epic2 for each input-ChIP pair. 1425 H3K4me1 peaks were identified in F9 ECCs within 1kb of previously annotated PpGe in ESCs (Whyte et

al., 2012). See also Figure S5A. Histone demethylation activity of Lsd1 was measured by calculating the change in H3K4me1 peak enrichment at PpGe between D4 differentiated and undifferentiated samples.

(A) Waterfall plot represents changes in H3K4me1, which were calculated as the difference between log2FC of D4 and undifferentiated samples and transformed to Z-score. Z-score thresholds of +1 and -1 were used to define the fractions showing increase, no change and decrease in H3K4me1 shown in the pie chart. Combined together 87% PpGe show an increase or no change (NDCM) in H3K4me1 enrichment.

(B, C) Venn diagram showing an overlap between PpGe that show (B) an increase, or (C) no change in peak enrichment in F9 ECCs but undergo histone H3K4me1 demethylation in ESCs post differentiation (Whyte et al., 2012).

(D) Top ten statistically significant enriched canonical pathways amongst the genes associated with increase and no change in F9 ECCs. The x-axis shows the $\log_{10}$(adjusted p-value), with the p-value adjusted for multiple testing using the Benjamini-Hochberg method.

(E) Overlap between the PpGe showing no change in DNA methylation (NDHM) and PpGe that show no decrease in H3K4me1 (NCDM).

**Figure 5. PpGe are decommissioned and in differentiating P19 ECCs**.

UD: undifferentiated; D4, D8: Days post induction of differentiation; P19 ECCs: P19 embryonal carcinoma cells, PpGs: pluripotency genes; PpGe: Pluripotency gene enhancers.

(A) Gene expression analysis by RT-qPCR of PpGs in P19 ECCs. The $C_t$ values for each gene were normalized to *Gapdh* and expression is shown relative to that in undifferentiated cells (dotted line). Similar to the repression of PpGs in ESCs (Figure 1A), PpGs, especially Oct4 and Nanog, show more than 90% reduction in expression.

(B) ChIP-qPCR showing H3K4me1 enrichment in UD and D4 differentiated P19 ECCs. A decrease in H3K4me1 was observed at all PpGe post differentiation showing histone demethylation activity.

(C) DNA methylation analysis of PpGe using Bis-Seq in UD, D4 and D8 differentiated P19 ECCs. A 40% increase in DNA methylation level was observed at PpGe post differentiation. Average and SEM of two biological replicates are shown for each gene.

**Figure 6. Oct4 directly interacts with Lsd1 and inhibits its catalytic activity.**

TCP: tranylcypromine; ECCs: embryonal carcinoma cells; PpGe: pluripotency gene enhancers D4: Days post induction of differentiation.

(A) GST-pull down experiment showing direct interaction between Lsd1 and Oct4. Recombinant GST-Lsd1 was incubated with Oct4 at about 1:2 molar ratio and precipitated using GST-Sepharose. The co-precipitated Oct4 is detected using Anti-Oct4 antibody.

(B) Lsd1 demethylase assay was performed using 0.25μM of Lsd1 and H3K4me2 peptide as substrate. Lsd1 demethylation activity was completely inhibited by 0.1mM TCP (tranylcypromine) in the reaction. To test the effect of Oct4 on Lsd1 activity, demethylation assays were performed in presence of 0.5μM Oct4 at 1:2 (Lsd1:Oct4) molar ratio. Catalytic domain of Dnmt3a at the same molar ratio was used as a control.

(C) Dose dependent inhibition assays were performed using increasing concentration of Oct4 in the following molar ratio of Lsd1:Oct4, (1:0.5), (1:1), (1:2), (1:3), (1:4). Data are an average and SD of at least 5 experimental replicates.

(D) Lsd1 demethylation assays were performed using 0.25μM of Lsd1 and 30μg bulk histones as substrate with increasing concentrations of Oct4 in the reaction. Upper Panel: Histone demethylation was detected by using anti H3K4me2 on Western blot showing a retention of

461 signal in presence of increasing concentration of Oct4. Lower panels: Amount of Lsd1 enzyme
462 and increasing amounts of Oct4 in the histone demethylation reaction. Ponceau S stain of bulk
463 histones shows equal loading on the gel.

464 (E) ChIP-qPCR showing percent enrichment of H3K4me1 at PpGe in P19 ECCs stably
465 expressing recombinant Myc-Oct4 pre- and post-differentiation. The data show retention of
466 H3K4me1 post differentiation.

467 (F) Gene expression analysis by RT-qPCR of PpGs in P19 ECCs expressing recombinant Myc-
468 Oct4. The $C_t$ values were normalized to *Gapdh* and expression is shown relative to that in
469 undifferentiated cells (dotted line).

470 (G) DNA methylation analysis of PpGe using Bis-Seq in UD and D4 differentiated P19 ECCs
471 WT and expressing recombinant Myc-Oct4. Oct4 expressing cells show failure to gain DNA
472 methylation at PpGe post differentiation compared to untransfected WT. Average and SEM of
473 two biological replicates are shown.

474 **Figure 7. Illustration of epigenetic state at PpGe in F9 ECCs during differentiation.**

475 In an undifferentiated state, the PpGe are active, bound by the coactivator complex and
476 chromatin modifications include H3K4m2/1 and H3K27Ac. In response to signal of
477 differentiation, the dissociation of the coactivator complex including Oct4 is followed by the
478 activity of the Lsd1-Mi2/NuRD complex, which facilitates enhancer silencing. The histone
479 deacetylase (HDAC) removes H3K27Ac at PpGe, and Lsd1 demethylates H3K4me1, followed
480 by DNA methylation by Dnmt3a. However, in F9 ECCs, Lsd1 activity is inhibited in presence of
481 Oct4 causing retention of H3K4me1. The ADD domain of Dnmt3a cannot interact with H3K4
482 methylated histone tail and will potentially remain in the autoinhibited state thus preventing DNA
483 methylation at these sites. Consequently, PpGe instead of being silenced acquire a “primed”
484 state. Black pins represent methylated CpGs.

## STAR Methods

### Cell culture and differentiation:

F9 embryonal carcinoma cells (F9 ECCs), P19 embryonal carcinoma cells (P19 ECCs), and E14Tg2A Embryonic stem cells (ESCs) were cultured and maintained in gelatin-coated tissue culture plates. Differentiation was induced by plating $20X10^6$ cells in low attachment 15 cm petri dishes and the addition of 1μM Retinoic acid (RA). ESCs were differentiated by the same method with a concurrent withdrawal of LIF. The medium was replenished every two days and samples were collected on Days 4, and 8 post differentiation.

Myc-Dnmt3a2 and FLAG-Lsd1 WT were transiently overexpressed in F9 ECCs using Lipofectamine 2000. One-day post transfection, a UD sample was collected (D0), and transfected cells were induced to differentiate on gelatinized plates by the addition of RA. The next day, differentiated cells were trypsinized and plated on low adherence petri dishes. Samples were collected on Days 4, and 8 post-differentiation. Lsd1 inhibitor treatment was performed as described 6 hrs prior to induction of differentiation (Petell et al., 2016).

P19 ECCs were transfected with Myc-Oct4 using Lipofectamine 2000 per the manufacturer's instructions. Transfected cells were clonally propagated, and Myc-Oct4 expression was determine by Western blots with anti-cMyc antibody (Millipore, MABE282).

### DNA methylation analysis

Bisulfite sequencing: Bisulfite conversion was performed using EpiTect Fast Bisulfite Conversion Kit (Qiagen, 59802) according to the manufacturer's protocol. PCR conditions for outer and inner amplifications were performed (Petell et al., 2016). The pooled samples were sequenced using NGS on Wide-Seq platform. The reads were assembled and analyzed by Bismark and Bowtie2. Methylated and unmethylated CpGs for each target were quantified, averaged, and presented as percent CpG methylation. Number of CpGs for regions tested are

509 listed in Supplementary table S1. Total number of reads used to calculate percent CpG
510 methylation are listed in Supplementary table S2. Primer sequences can be found in
511 Supplementary table S4.

512 MethylRAD sequencing: Genomic DNA was isolated using a standard phenol:chloroform
513 extraction, followed by ethanol precipitation. DNA from various samples was digested with
514 FspEI overnight at 37°C and run on 2% agarose gel. 30 base pair fragments were cut out,
515 purified and adaptor ligated at 4°C overnight (Wang et al., 2015b). The ligated DNA was PCR
516 amplified with index primers and sequenced in Novaseq2000. The primers used for PCR
517 amplification is in Supplementary table S4. The details of the bioinformatics analysis of data are
518 in Supplementary Methods.

519 **Chromatin Immunoprecipitation and ChIP-Seq**

520 ChIP was performed as described (Petell et al., 2016). Chromatin was sheared by sonication
521 using Covaris E210 device, according to the manufacturer's protocol. 8µg of sheared
522 crosslinked chromatin was incubated with 8µg of antibody pre-loaded on 1:1 ratio of protein A
523 and protein G magnetic beads (Life Technologies, 10002D and 10004D, respectively). After
524 washing the beads, the samples were eluted in 1% SDS, 10 mM EDTA, 50 mM Tris-HCl, pH
525 8.0. Crosslinking was reversed by incubation at 65°C for 30 min with shaking. Samples were
526 treated with RNase (Roche, 11119915001) for 2 h at 37°C, and subsequently treated with
527 Proteinase K (Worthington, LS004222) for 2 h at 55°C. DNA was purified by Phenol:Chloroform
528 extraction followed by ethanol precipitation and quantified using PicoGreen (Life Technologies,
529 P11495) and NanoDrop 3300 fluorospectrometer. qPCR was then performed using equal
530 amounts of IN and IP samples. Fold enrichment was calculated as: $2^{( C_t(IN)-C_t(IP))}$.
531 Supplementary Table S4 lists sequences of primers used.

## Gene expression analysis

RNA was isolated by TRIzol (Invitrogen, 15596026) according to manufacturer's protocol. Samples were treated with DNAse (Roche, 04716728001) at 37°C, and then purified using Quick-RNA™ MiniPrep Plus Kit (ZymoReseach, R1057). Reverse-transcription quantitative PCR was performed by using Verso One-Step RT-qPCR kits (Thermo Scientific, AB-4104A) with 1µg of purified RNA. Gene expression was calculated as $\Delta C_t$ which is $C_t$(Gene)- $C_t$(*Gapdh*). Change in gene expression is reported as fold change relative to that in undifferentiated cells, which was set to 1. See Supplementary table S4 for primers used.

## Microscopy

Bright field images of Embryoid bodies (EBs) were obtained with Zeiss microscope at 10X objective. Alkaline phosphatase staining was performed using solutions supplied by an alkaline phosphatase staining kit (Sigma, AB0300). Cells were cross-linked with 1% formaldehyde for 5 min, followed by quenching with a final concentration of 150 mM Glycine. Cells were washed twice with 1xPBS, then twice with combined staining solution (BCIP and NBT). The stain was developed in the dark for 5 min, then washed three times with 1x PBS. SSEA-1 immunofluorescence was performed using the following antibodies: anti-SSEA-1 (Millipore, MAB430) and AlexaFluor 555 nm (Life Technologies, A21422). SSEA-1 and Alkaline phosphatase staining were imaged using 20X objectives under Nikon Ts and Zeiss microscopes, respectively.

## Co-precipitation experiment

Immunoprecipitation assays were performed with 1µg of GST-Lsd1 (Sigma, SRP0122) incubated with 1µg of recombinant Oct4 (abcam, ab134876) and Glutathione sepharose 4B (GE healthcare, 17-0756-01) resin in binding buffer (50mM Tris pH8.5, 50mM KCl, 5mM MgCl, 0.5% BSA, and 5% glycerol, complemented with a cocktail of protease inhibitors) overnight at 4°C

with gentle agitation. The resin was washed twice with binding buffer and proteins were eluted elution buffer (50mM Tris-HCl, 10mM reduced glutathione, pH8) according to manufacturer's instructions. Eluate and input were loaded onto 10% SDS-PAGE gels and blots were probed using anti-Lsd1 (abcam, ab17721) and anti-Oct4 (Santa Cruz, sc-8628) antibodies.

### *In vitro* Lsd1 demethylase activity assay

*In vitro* fluorometric assay were performed using Lsd1 demethylase activity assay, Epigenase™ kit (Epigentek, P-0379) according to manufacturer's protocol. 0.25μM of Lsd1 (Sigma, SRP0122) was used together with 0.5μM (or as indicated) of Oct4 (abcam, ab134876 and ab169842) or BSA (Sigma, A3059) or catalytic domain of Dnmt3a (*purified in house*) or 0.1mM Lsd1 inhibitor Tranylcypromine (TCP). Signals were measured using CLARIOstar plate reader and analyzed using MARs software as described by the manufacturer.

### Histone demethylation assay

Lsd1 histone demethylation assays were performed as described in (Shi et al., 2004). 30μg of bulk histones (Sigma, H9250) in a histone demethylation buffer (50mM Tris pH8.5, 50mM KCl, 5mM MgCl, 0.5% BSA, and 5% glycerol) were incubated with 0.25μM of Lsd1 (Sigma, SRP0122) alone, or increasing concentrations (0.125μM, 0.25μM, 0.5μM, 1μM) of Oct4 (abcam, ab134876 and ab169842), or 0.1μM TCP for 4 hrs at 37°C. Lsd1 activity was monitored by Western blot using anti-H3K4me2 antibody (abcam, ab32356). The membrane was stained by Ponceau S to detect equal loading of the reaction mix.

## Supplemental Figure legends

### Figure S1. Expression of epigenetic effectors in F9 ECCs.

UD: undifferentiated, D4: Days post differentiation. ESCs: embryonic stem cells and F9 ECCs: F9 embryonal carcinoma cells; PpGe: pluripotency gene enhancers.

(A and B) Bis-Seq analysis of DNA methylation at PpG (A) enhancers and (B) promoters in F9 ECCs pre- and post-differentiation. The DNA methylation at PpGe remained under 10% even at 6 days post differentiation. DNA methylation at PpG promoters is also low except *Lefty2*, which shows very high methylation in the UD state that is reduced post differentiation.

(C) RT-qPCR comparing the changes in expression of DNA methyltransferase Dnmt3a and histone demethylase Lsd1 in ESCs with that in F9 ECCs pre- and post-differentiation. The $C_t$ values are normalized to *Gapdh* and represented relative to expression in undifferentiated cells (dotted line). In both ESCs and ECCs, Lsd1 and Dnmt3a expression is maintained post differentiation.

(D) Western blot. 50 µgs of total cell extract from undifferentiated and differentiated cells were loaded in each well. Left panel confirms comparable expression of Dnmt3a and Lsd1 pre- and post-differentiation in F9 ECCs. Right panel compares Lsd1 expression in F9 ECCs with ESCs showing very similar levels in these cells. β-Actin is the loading control.

(E) Gene expression analysis by RT-qPCR and Western blot confirming recombinant Myc-Dnmt3a overexpression in F9 ECCs 24 hrs post differentiation (48 hrs post transfection). The data are normalized to *Gapdh* control and shown relative to untransfected that is set to 1. β-Actin is used as loading control for Western blot.

**Figure S2. Distribution of MethylRAD peaks.**

(A) Fractional distribution of MethylRAD peaks in undifferentiated and differentiated F9 ECCs across regulatory regions of the genome.

(B) Pie charts show the level of methylation at PpGe in undifferentiated (grey) and differentiated day 4 (blue) samples. Most PpGe had low levels of methylation or to a lesser extent, intermediate levels of methylation, with none having high CpG methylation.

**Figure S3. H3K27 modification of PpGe in ESCs and F9 ECCs.**

UD: undifferentiated; D4: Days post induction of differentiation; IP: immunoprecipitation

(A, B, and C) ChIP-qPCR was used to determine the percent enrichment of histone modifications at PpGe. (A) H3K27Ac in ESCs (B) H3K27me3 in ESCs and (C) H3K27me3 in F9 ECCs pre- and post-differentiation. Whereas deacetylation of PpGe is observed as a decrease in H3K27Ac signal post differentiation in ESCs, there is no gain of H3K27me3 at these sites neither in ESCs, no in F9 ECCs. A previously reported, we observed a decrease in H3K27me3 at the enhancers and promoters of *Hoxa5* and *mNr2f1* genes, consistent with their transcriptional activation in response to differentiation (Laursen et al., 2013)

(D) Co-IP was performed with anti-Lsd1, and anti-HDAC1 using whole cell extracts from undifferentiated ESCs and F9 ECCs. 20% input and eluate from Co-IP was probed for Lsd1-Mi2/NuRD subunits (Lsd1, HDAC1 and CHD4) on Western blot.

**Figure S4. Overexpression or inhibition of Lsd1 has little to no effect on differentiation and PpGe silencing in F9 ECCs.**

UD: undifferentiated; D8: Days post induction of differentiation; Prg: pargyline; TCP: Tranylcypromine.

(A) Gene expression analysis by RT-qPCR and Western blot examining the expression of recombinant FLAG-Lsd1 in F9 ECCs 24 hrs post differentiation (48 hrs post transfection). The $C_t$ values are normalized to *Gapdh* and represented relative to expression in untransfected cells (set to 1). β-Actin is used as loading control for Western blot

(B) Gene expression analysis by RT-qPCR of PpGs in F9 ECCs expressing FLAG-Lsd1.Similar to untransfected WT F9 ECCs, PpGs are partially repressed in these cells showing no effect of recombinant Lsd1 on PpG repression.

(C) Bis-Seq analysis of DNA methylation at PpGe in F9 ECCs expressing recombinant FLAG-Lsd1 showed no gain corresponding to no loss of H3K4me1 at these sites. Data are an average and SEM of two biological replicates.

(D) Bright field microscopy of ESCs, and ECCs differentiated for 4 days in presence of Lsd1 inhibitors, Prg or TCP. 80-90% cell death is observed in ESCs, Lsd1 inhibitors have no effect on F9 ECC differentiation as shown by a normal morphology of embryoid bodies. Scale bar is 100μm.

(E) Gene expression analysis of PpGs by RT-qPCR in differentiating F9 ECCs; untreated and treated with Prg and TCP. A slight derepression of PpGs was observed in inhibitor treated cells post differentiation. Gene expression was normalized to *Gapdh* and represented as relative change to gene expression in undifferentiated (dotted line).

(F) Undifferentiated F9 ECCs were transfected with FLAG-Lsd1 and cultured for 72 hrs. H3K4me1 enrichment was determined using ChIP-qPCR. No change in H3K4me1 levels was observed compared untransfected (UT) cells.

**Figure S5. Distribution of H3K4me1 ChIP-Seq peaks.**

(A) Summary of the overlapping LSD1 bound sites between H3K4me1 peaks in F9 ECCs and ESCs (Whyte et al., 2012). To determine correct overlap, Whyte et al peak coordinates were converted from mm8 to mm10 using CrossMap tool (Zhao et al., 2014).

(B) Fractional distribution of H3K4me1 peaks in undifferentiated and differentiated F9 ECCs throughout the genome.

(C) Overlap of the sites that show decrease in H3K4me1 post-differentiation in ESCs (Whyte et al., 2012), and F9 ECCs.

(D) Top ten most statistically significant enriched canonical pathways amongst the genes associated with decrease in F9 ECCs.

**Figure S6. P19 ECCs are sensitive to Lsd1 inhibitor.**

D4: Days post induction of differentiation; Prg: pargyline; UT: untransfected control.

(A) Bright field microscopy of P19 ECCs differentiated for 4 days in presence of Lsd1 inhibitor, Prg. 80-90% cell death is observed in P19 ECCs indicating that Lsd1 activity at PpGe is required for differentiation. Scale bar is 100μm.

(C) Expression analysis by Western blot confirming recombinant Myc-Oct4 overexpression in two independent clones of P19 ECCs. β-Actin is used as loading control for Western blot.

**Table S1. Number of CpGs at each site used for Bis-Seq DNA methylation analysis.**

The number of CpGs sites used to compute percent methylation within H19 imprinted region in addition to PpG enhancers, and promoters in bisulfite-sequencing analyses.

659 **Table S2. Number of reads for each enhancer used for Bis-Seq analysis.**

660 The total number of reads from Wide-Seq runs that were used for data presented in this study.
661 The number of reads were calculated for each sample, enhancer, along with the overall total
662 reads.

663 **Table S3. Number of reads for promoters and imprinted region used for Bis-Seq analysis.**

664 The total number of reads from Wide-Seq runs that were used in this study. The number of
665 reads were calculated for each sample, promoter site, imprinted locus as well as the overall total
666 reads.

667 **Table S4. Primers used in this study.**

668 A list of all PCR primers used in this study (5' to 3'), separated by technique. The presence of
669 (AminoC6) modification at 3' end of the antisense oligonucleotide of each adaptor is used to
670 block extension.

## References


AKHTAR-ZAIDI, B., COWPER-SAL, R., CORRADIN, O., SAIAKHOVA, A., BARTELS, C. F., BALASUBRAMANIAN, D., MYEROFF, L., LUTTERBAUGH, J., JARRAR, A. & KALADY, M. F. 2012. Epigenomic enhancer profiling defines a signature of colon cancer. *Science,* 336**,** 736-739.

ALONSO, A., BREUER, B., STEUER, B. & FISCHER, J. 1991. The F9-EC cell line as a model for the analysis of differentiation. *Int J Dev Biol,* 35**,** 389-97.

ANDREWS, P. W., MATIN, M. M., BAHRAMI, A. R., DAMJANOV, I., GOKHALE, P. & DRAPER, J. S. 2005. Embryonic stem (ES) cells and embryonal carcinoma (EC) cells: Opposite sides of the same coin. *Biochemical Society Transactions,* 33**,** 1526-1530.

ARAN, D. & HELLMAN, A. 2013. DNA methylation of transcriptional enhancers and cancer predisposition. *Cell,* 154**,** 11-13.

ARAN, D., SABATO, S. & HELLMAN, A. 2013. DNA methylation of distal regulatory sites characterizes dysregulation of cancer genes. *Genome biology,* 14**,** R21.

BANERJI, J., RUSCONI, S. & SCHAFFNER, W. 1981. Expression of a beta-globin gene is enhanced by remote SV40 DNA sequences. *Cell,* 27**,** 299-308.

BARON, R., BINDA, C., TORTORICI, M., MCCAMMON, J. A. & MATTEVI, A. 2011. Molecular mimicry and ligand recognition in binding and catalysis by the histone demethylase LSD1-CoREST complex. *Structure,* 19**,** 212-20.

BARSKI, A., CUDDAPAH, S., CUI, K., ROH, T.-Y., SCHONES, D. E., WANG, Z., WEI, G., CHEPELEV, I. & ZHAO, K. 2007. High-resolution profiling of histone methylations in the human genome. *Cell,* 129**,** 823-837.

BEN-PORATH, I., THOMSON, M. W., CAREY, V. J., GE, R., BELL, G. W., REGEV, A. & WEINBERG, R. A. 2008. An embryonic stem cell-like gene expression signature in poorly differentiated aggressive human tumors. *Nat Genet,* 40**,** 499-507.

BULGER, M. & GROUDINE, M. 2011. Functional and mechanistic diversity of distal transcription enhancers. *Cell,* 144**,** 327-339.

CALO, E. & WYSOCKA, J. 2013. Modification of enhancer chromatin: what, how, and why? *Mol Cell,* 49**,** 825-837.

CARNESECCHI, J., FORCET, C., ZHANG, L., TRIBOLLET, V., BARENTON, B., BOUDRA, R., CERUTTI, C., BILLAS, I. M., SERANDOUR, A. A., CARROLL, J. S., BEAUDOIN, C. & VANACKER, J. M. 2017. ERRalpha induces H3K9 demethylation by LSD1 to promote cell invasion. *Proc Natl Acad Sci U S A,* 114**,** 3909-3914.

CHAPUY, B., MCKEOWN, M. R., LIN, C. Y., MONTI, S., ROEMER, M. G., QI, J., RAHL, P. B., SUN, H. H., YEDA, K. T., DOENCH, J. G., REICHERT, E., KUNG, A. L., RODIG, S. J., YOUNG, R. A., SHIPP, M. A. & BRADNER, J. E. 2013. Discovery and characterization of super-enhancer-associated dependencies in diffuse large B cell lymphoma. *Cancer Cell,* 24**,** 777-90.

COHEN-KARNI, D., XU, D., APONE, L., FOMENKOV, A., SUN, Z., DAVIS, P. J., KINNEY, S. R., YAMADA-MABUCHI, M., XU, S. Y., DAVIS, T., PRADHAN, S., ROBERTS, R. J. & ZHENG, Y. 2011. The MspJI family of modification-dependent restriction endonucleases for epigenetic studies. *Proc Natl Acad Sci U S A,* 108**,** 11040-5.

CREYGHTON, M. P., CHENG, A. W., WELSTEAD, G. G., KOOISTRA, T., CAREY, B. W., STEINE, E. J., HANNA, J., LODATO, M. A., FRAMPTON, G. M. & SHARP, P. A. 2010. Histone H3K27ac separates active from poised enhancers and predicts developmental state. *Proceedings of the National Academy of Sciences,* 107**,** 21931-21936.

DE THE, H. 2018. Differentiation therapy revisited. *Nat Rev Cancer,* 18**,** 117-127.

716 ERNST, J. & KELLIS, M. 2010. Discovery and characterization of chromatin states for systematic
717 annotation of the human genome. *Nat Biotechnol,* 28**,** 817.
718 ERNST, J., KHERADPOUR, P., MIKKELSEN, T. S., SHORESH, N., WARD, L. D., EPSTEIN, C. B., ZHANG, X.,
719 WANG, L., ISSNER, R. & COYNE, M. 2011. Mapping and analysis of chromatin state dynamics in
720 nine human cell types. *Nature,* 473**,** 43.
721 FESKE, S. 2007. Calcium signalling in lymphocyte activation and disease. *Nat Rev Immunol,* 7**,** 690-702.
722 GAO, X. N., YAN, F., LIN, J., GAO, L., LU, X. L., WEI, S. C., SHEN, N., PANG, J. X., NING, Q. Y., KOMENO, Y.,
723 DENG, A. L., XU, Y. H., SHI, J. L., LI, Y. H., ZHANG, D. E., NERVI, C., LIU, S. J. & YU, L. 2015.
724 AML1/ETO cooperates with HIF1alpha to promote leukemogenesis through DNMT3a
725 transactivation. *Leukemia,* 29**,** 1730-40.
726 GORDEEVA, O. & KHAYDUKOV, S. 2017. Tumorigenic and Differentiation Potentials of Embryonic Stem
727 Cells Depend on TGFβ Family Signaling: Lessons from Teratocarcinoma Cells Stimulated to
728 Differentiate with Retinoic Acid. *Stem cells international,* 2017.
729 GROSCHEL, S., SANDERS, M. A., HOOGENBOEZEM, R., DE WIT, E., BOUWMAN, B. A., ERPELINCK, C., VAN
730 DER VELDEN, V. H., HAVERMANS, M., AVELLINO, R., VAN LOM, K., ROMBOUTS, E. J., VAN DUIN,
731 M., DOHNER, K., BEVERLOO, H. B., BRADNER, J. E., DOHNER, H., LOWENBERG, B., VALK, P. J.,
732 BINDELS, E. M., DE LAAT, W. & DELWEL, R. 2014. A single oncogenic enhancer rearrangement
733 causes concomitant EVI1 and GATA2 deregulation in leukemia. *Cell,* 157**,** 369-81.
734 GWAK, J. M., KIM, M., KIM, H. J., JANG, M. H. & PARK, S. Y. 2017. Expression of embryonal stem cell
735 transcription factors in breast cancer: Oct4 as an indicator for poor clinical outcome and
736 tamoxifen resistance. *Oncotarget,* 8**,** 36305-36318.
737 HAN, J. W., GURUNATHAN, S., CHOI, Y. J. & KIM, J. H. 2017. Dual functions of silver nanoparticles in F9
738 teratocarcinoma stem cells, a suitable model for evaluating cytotoxicity- and differentiation-
739 mediated cancer therapy. *International Journal of Nanomedicine,* 12**,** 7529-7549.
740 HEINTZMAN, N. D., STUART, R. K., HON, G., FU, Y., CHING, C. W., HAWKINS, R. D., BARRERA, L. O., VAN
741 CALCAR, S., QU, C. & CHING, K. A. 2007. Distinct and predictive chromatin signatures of
742 transcriptional promoters and enhancers in the human genome. *Nat Genet,* 39**,** 311.
743 HEINZ, S., BENNER, C., SPANN, N., BERTOLINO, E., LIN, Y. C., LASLO, P., CHENG, J. X., MURRE, C., SINGH,
744 H. & GLASS, C. K. 2010. Simple combinations of lineage-determining transcription factors prime
745 cis-regulatory elements required for macrophage and B cell identities. *Mol Cell,* 38**,** 576-589.
746 HEINZ, S., ROMANOSKI, C. E., BENNER, C. & GLASS, C. K. 2015. The selection and function of cell type-
747 specific enhancers. *Nat Rev Mol Cell Biol,* 16**,** 144-54.
748 HNISZ, D., SCHUIJERS, J., LIN, C. Y., WEINTRAUB, A. S., ABRAHAM, B. J., LEE, T. I., BRADNER, J. E. &
749 YOUNG, R. A. 2015. Convergence of developmental and oncogenic signaling pathways at
750 transcriptional super-enhancers. *Mol Cell,* 58**,** 362-70.
751 HOSSEINI, A. & MINUCCI, S. 2017. A comprehensive review of lysine-specific demethylase 1 and its roles
752 in cancer. *Epigenomics,* 9**,** 1123-1142.
753 IGLESIAS, J. M., GUMUZIO, J. & MARTIN, A. G. 2017. Linking Pluripotency Reprogramming and Cancer.
754 *Stem Cells Transl Med,* 6**,** 335-339.
755 JETER, C. R., LIU, B., LIU, X., CHEN, X., LIU, C., CALHOUN-DAVIS, T., REPASS, J., ZAEHRES, H., SHEN, J. J. &
756 TANG, D. G. 2011. NANOG promotes cancer stem cell characteristics and prostate cancer
757 resistance to androgen deprivation. *Oncogene,* 30**,** 3833-45.
758 JONES, P. A., ISSA, J.-P. J. & BAYLIN, S. 2016. Targeting the cancer epigenome for therapy. *Nature*
759 *Reviews Genetics,* 17**,** 630.
760 KASHYAP, V., AHMAD, S., NILSSON, E. M., HELCZYNSKI, L., KENNA, S., PERSSON, J. L., GUDAS, L. J. &
761 MONGAN, N. P. 2013. The lysine specific demethylase-1 (LSD1/KDM1A) regulates VEGF-A
762 expression in prostate cancer. *Mol Oncol,* 7**,** 555-66.

763 KIM, B. W., CHO, H., CHOI, C. H., YLAYA, K., CHUNG, J. Y., KIM, J. H. & HEWITT, S. M. 2015. Clinical
764 significance of OCT4 and SOX2 protein expression in cervical cancer. *BMC Cancer,* 15**,** 1015.
765 KNOECHEL, B., RODERICK, J. E., WILLIAMSON, K. E., ZHU, J., LOHR, J. G., COTTON, M. J., GILLESPIE, S. M.,
766 FERNANDEZ, D., KU, M. & WANG, H. 2014. An epigenetic mechanism of resistance to targeted
767 therapy in T cell acute lymphoblastic leukemia. *Nature genetics,* 46**,** 364.
768 KUMAR, S. M., LIU, S., LU, H., ZHANG, H., ZHANG, P. J., GIMOTTY, P. A., GUERRA, M., GUO, W. & XU, X.
769 2012. Acquired cancer stem cell phenotypes through Oct4-mediated dedifferentiation.
770 *Oncogene,* 31**,** 4898-911.
771 LAURENT, B., RUITU, L., MURN, J., HEMPEL, K., FERRAO, R., XIANG, Y., LIU, S., GARCIA, B. A., WU, H., WU,
772 F., STEEN, H. & SHI, Y. 2015. A specific LSD1/KDM1A isoform regulates neuronal differentiation
773 through H3K9 demethylation. *Mol Cell,* 57**,** 957-970.
774 LAURSEN, K. B., MONGAN, N. P., ZHUANG, Y., NG, M. M., BENOIT, Y. D. & GUDAS, L. J. 2013. Polycomb
775 recruitment attenuates retinoic acid-induced transcription of the bivalent NR2F1 gene. *Nucleic*
776 *Acids Res,* 41**,** 6430-43.
777 LI, J. Y., PU, M. T., HIRASAWA, R., LI, B. Z., HUANG, Y. N., ZENG, R., JING, N. H., CHEN, T., LI, E., SASAKI, H.
778 & XU, G. L. 2007. Synergistic function of DNA Methyltransferases dnmt3a and dnrnt3b in the
779 methylation of Oct4 and Nanog. *Molecular and Cellular Biology,* 27**,** 8748-8759.
780 LINDROTH, A. M., PARK, Y. J., MCLEAN, C. M., DOKSHIN, G. A., PERSSON, J. M., HERMAN, H., PASINI, D.,
781 MIRO, X., DONOHOE, M. E. & LEE, J. T. 2008. Antagonism between DNA and H3K27 methylation
782 at the imprinted Rasgrf1 locus. *PLoS genetics,* 4**,** e1000145.
783 LINN, D. E., YANG, X., SUN, F., XIE, Y., CHEN, H., JIANG, R., CHUMSRI, S., BURGER, A. M. & QIU, Y. 2010. A
784 Role for OCT4 in Tumor Initiation of Drug-Resistant Prostate Cancer Cells. *Genes Cancer,* 1**,** 908-
785 16.
786 LIU, A., YU, X. & LIU, S. 2013. Pluripotency transcription factors and cancer stem cells: small genes make
787 a big difference. *Chin J Cancer,* 32**,** 483-7.
788 LOVEN, J., HOKE, H. A., LIN, C. Y., LAU, A., ORLANDO, D. A., VAKOC, C. R., BRADNER, J. E., LEE, T. I. &
789 YOUNG, R. A. 2013. Selective inhibition of tumor oncogenes by disruption of super-enhancers.
790 *Cell,* 153**,** 320-34.
791 LV, T., YUAN, D., MIAO, X., LV, Y., ZHAN, P., SHEN, X. & SONG, Y. 2012. Over-expression of LSD1
792 promotes proliferation, migration and invasion in non-small cell lung cancer. *PLoS One,* 7**,**
793 e35065.
794 MA, H. S., WANG, E. L., XU, W. F., YAMADA, S., YOSHIMOTO, K., QIAN, Z. R., SHI, L., LIU, L. L. & LI, X. H.
795 2018. Overexpression of DNA (Cytosine-5)-Methyltransferase 1 (DNMT1) And DNA (Cytosine-5)-
796 Methyltransferase 3A (DNMT3A) Is Associated with Aggressive Behavior and Hypermethylation
797 of Tumor Suppressor Genes in Human Pituitary Adenomas. *Med Sci Monit,* 24**,** 4841-4850.
798 MAGNANI, L., STOECK, A., ZHANG, X., LÁNCZKY, A., MIRABELLA, A. C., WANG, T.-L., GYORFFY, B. &
799 LUPIEN, M. 2013. Genome-wide reprogramming of the chromatin landscape underlies
800 endocrine therapy resistance in breast cancer. *Proceedings of the National Academy of Sciences***,**
801 201219992.
802 MAK, V. C., SIU, M. K., WONG, O. G., CHAN, K. K., NGAN, H. Y. & CHEUNG, A. N. 2012. Dysregulated
803 stemness-related genes in gynecological malignancies. *Histol Histopathol,* 27**,** 1121-30.
804 MANSOUR, M. R., ABRAHAM, B. J., ANDERS, L., BEREZOVSKAYA, A., GUTIERREZ, A., DURBIN, A. D.,
805 ETCHIN, J., LAWTON, L., SALLAN, S. E., SILVERMAN, L. B., LOH, M. L., HUNGER, S. P., SANDA, T.,
806 YOUNG, R. A. & LOOK, A. T. 2014. Oncogene regulation. An oncogenic super-enhancer formed
807 through somatic mutation of a noncoding intergenic element. *Science,* 346**,** 1373-7.
808 MCCLELLAN, D., CASEY, M. J., BAREYAN, D., LUCENTE, H., OURS, C., VELINDER, M., SINGER, J., LONE, M.
809 D., SUN, W., CORIA, Y., MASON, C. & ENGEL, M. E. 2019. Growth Factor Independence (GFI) 1B-

mediated transcriptional repression and lineage allocation require Lysine Specific Demethylase (LSD)1-dependent recruitment of the BHC complex. *Mol Cell Biol*.

MENDENHALL, E. M., WILLIAMSON, K. E., REYON, D., ZOU, J. Y., RAM, O., JOUNG, J. K. & BERNSTEIN, B. E. 2013. Locus-specific editing of histone modifications at endogenous enhancers. *Nat Biotechnol,* 31**,** 1133-6.

METZGER, E., WISSMANN, M., YIN, N., MULLER, J. M., SCHNEIDER, R., PETERS, A. H., GUNTHER, T., BUETTNER, R. & SCHULE, R. 2005. LSD1 demethylates repressive histone marks to promote androgen-receptor-dependent transcription. *Nature,* 437**,** 436-9.

ONG, C.-T. & CORCES, V. G. 2011. Enhancer function: new insights into the regulation of tissue-specific gene expression. *Nature Reviews Genetics,* 12**,** 283.

PARDO, M., LANG, B., YU, L., PROSSER, H., BRADLEY, A., BABU, M. M. & CHOUDHARY, J. 2010. An expanded Oct4 interaction network: implications for stem cell biology, development, and disease. *Cell Stem Cell,* 6**,** 382-95.

PENG, S., MAIHLE, N. J. & HUANG, Y. 2010. Pluripotency factors Lin28 and Oct4 identify a sub-population of stem cell-like cells in ovarian cancer. *Oncogene,* 29**,** 2153-9.

PETELL, C. J., ALABDI, L., HE, M., SAN MIGUEL, P., ROSE, R. & GOWHER, H. 2016. An epigenetic switch regulates de novo DNA methylation at a subset of pluripotency gene enhancers during embryonic stem cell differentiation. *Nucleic Acids Res,* 44**,** 7605-17.

PLANK, J. L. & DEAN, A. 2014. Enhancer function: mechanistic and genome-wide insights come together. *Mol Cell,* 55**,** 5-14.

RADA-IGLESIAS, A., BAJPAI, R., SWIGUT, T., BRUGMANN, S. A., FLYNN, R. A. & WYSOCKA, J. 2011. A unique chromatin signature uncovers early developmental enhancers in humans. *Nature,* 470**,** 279.

SAMPIERI, K. & FODDE, R. 2012. Cancer stem cells and metastasis. *Semin Cancer Biol,* 22**,** 187-93.

SCHOENHALS, M., KASSAMBARA, A., DE VOS, J., HOSE, D., MOREAUX, J. & KLEIN, B. 2009. Embryonic stem cell markers expression in cancers. *Biochem Biophys Res Commun,* 383**,** 157-62.

SCHÜBELER, D. 2015. Function and information content of DNA methylation. *Nature,* 517**,** 321.

SHI, Y., LAN, F., MATSON, C., MULLIGAN, P., WHETSTINE, J. R., COLE, P. A., CASERO, R. A. & SHI, Y. 2004. Histone demethylation mediated by the nuclear amine oxidase homolog LSD1. *Cell,* 119**,** 941-53.

SHI, Y. J., MATSON, C., LAN, F., IWASE, S., BABA, T. & SHI, Y. 2005. Regulation of LSD1 histone demethylase activity by its associated factors. *Mol Cell,* 19**,** 857-64.

SPERANZINI, V., CIOSSANI, G., MARABELLI, C. & MATTEVI, A. 2017. Probing the interaction of the p53 C-terminal domain to the histone demethylase LSD1. *Arch Biochem Biophys,* 632**,** 202-208.

TABERLAY, P. C., STATHAM, A. L., KELLY, T. K., CLARK, S. J. & JONES, P. A. 2014. Reconfiguration of nucleosome-depleted regions at distal regulatory elements accompanies DNA methylation of enhancers and insulators in cancer. *Genome research***,** gr. 163485.113.

VAN DEN BERG, D. L. C., SNOEK, T., MULLIN, N. P., YATES, A., BEZSTAROSTI, K., DEMMERS, J., CHAMBERS, I. & POOT, R. A. 2010. An Oct4-Centered Protein Interaction Network in Embryonic Stem Cells. *Cell Stem Cell,* 6**,** 369-381.

VINYARD, M. E., SU, C., SIEGENFELD, A. P., WATERBURY, A. L., FREEDY, A. M., GOSAVI, P. M., PARK, Y., KWAN, E. E., SENZER, B. D., DOENCH, J. G., BAUER, D. E., PINELLO, L. & LIAU, B. B. 2019. CRISPR-suppressor scanning reveals a nonenzymatic role of LSD1 in AML. *Nat Chem Biol,* 15**,** 529-539.

WANG, J., TELESE, F., TAN, Y., LI, W., JIN, C., HE, X., BASNET, H., MA, Q., MERKURJEV, D., ZHU, X., LIU, Z., ZHANG, J., OHGI, K., TAYLOR, H., WHITE, R. R., TAZEARSLAN, C., SUH, Y., MACFARLAN, T. S., PFAFF, S. L. & ROSENFELD, M. G. 2015a. LSD1n is an H4K20 demethylase regulating memory formation via transcriptional elongation control. *Nat Neurosci,* 18**,** 1256-64.

WANG, S., LV, J., ZHANG, L., DOU, J., SUN, Y., LI, X., FU, X., DOU, H., MAO, J., HU, X. & BAO, Z. 2015b. MethylRAD: a simple and scalable method for genome-wide DNA methylation profiling using methylation-dependent restriction enzymes. *Open Biol,* 5.

WANG, X. Q., ONGKEKO, W. M., CHEN, L., YANG, Z. F., LU, P., CHEN, K. K., LOPEZ, J. P., POON, R. T. & FAN, S. T. 2010. Octamer 4 (Oct4) mediates chemotherapeutic drug resistance in liver cancer cells through a potential Oct4-AKT-ATP-binding cassette G2 pathway. *Hepatology,* 52**,** 528-39.

WANG, Y., ZHANG, H., CHEN, Y., SUN, Y., YANG, F., YU, W., LIANG, J., SUN, L., YANG, X., SHI, L., LI, R., LI, Y., ZHANG, Y., LI, Q., YI, X. & SHANG, Y. 2009. LSD1 is a subunit of the NuRD complex and targets the metastasis programs in breast cancer. *Cell,* 138**,** 660-72.

WANG, Y. D., CAI, N., WU, X. L., CAO, H. Z., XIE, L. L. & ZHENG, P. S. 2013. OCT4 promotes tumorigenesis and inhibits apoptosis of cervical cancer cells by miR-125b/BAK1 pathway. *Cell Death Dis,* 4**,** e760.

WANG, Z., ZANG, C., ROSENFELD, J. A., SCHONES, D. E., BARSKI, A., CUDDAPAH, S., CUI, K., ROH, T.-Y., PENG, W. & ZHANG, M. Q. 2008. Combinatorial patterns of histone acetylations and methylations in the human genome. *Nature genetics,* 40**,** 897.

WEN, J., PARK, J. Y., PARK, K. H., CHUNG, H. W., BANG, S., PARK, S. W. & SONG, S. Y. 2010. Oct4 and Nanog expression is associated with early stages of pancreatic carcinogenesis. *Pancreas,* 39**,** 622-6.

WHYTE, W. A., BILODEAU, S., ORLANDO, D. A., HOKE, H. A., FRAMPTON, G. M., FOSTER, C. T., COWLEY, S. M. & YOUNG, R. A. 2012. Enhancer decommissioning by LSD1 during embryonic stem cell differentiation. *Nature,* 482**,** 221-5.

YANG, F., ZHANG, J. & YANG, H. 2018. OCT4, SOX2, and NANOG positive expression correlates with poor differentiation, advanced disease stages, and worse overall survival in HER2(+) breast cancer patients. *Onco Targets Ther,* 11**,** 7873-7881.

YEGNASUBRAMANIAN, S., WU, Z., HAFFNER, M. C., ESOPI, D., ARYEE, M. J., BADRINATH, R., HE, T. L., MORGAN, J. D., CARVALHO, B. & ZHENG, Q. 2011. Chromosome-wide mapping of DNA methylation patterns in normal and malignant prostate cells reveals pervasive methylation of gene-associated and conserved intergenic sequences. *BMC genomics,* 12**,** 313.

YU, Z., XIAO, Q., ZHAO, L., REN, J., BAI, X., SUN, M., WU, H., LIU, X., SONG, Z., YAN, Y., MI, X., WANG, E., JIN, F. & WEI, M. 2015. DNA methyltransferase 1/3a overexpression in sporadic breast cancer is associated with reduced expression of estrogen receptor-alpha/breast cancer susceptibility gene 1 and poor prognosis. *Mol Carcinog,* 54**,** 707-19.

ZARET, K. S. & CARROLL, J. S. 2011. Pioneer transcription factors: establishing competence for gene expression. *Genes Dev,* 25**,** 2227-41.

ZENTNER, G. E., TESAR, P. J. & SCACHERI, P. C. 2011. Epigenetic signatures distinguish multiple classes of enhancers with distinct cellular functions. *Genome Res*.

ZHANG, X. M., LU, F., WANG, J., YIN, F., XU, Z. S., QI, D. D., WU, X. H., CAO, Y. W., LIANG, W. H., LIU, Y. Q., SUN, H., YE, T. & ZHANG, H. 2013. Pluripotent Stem Cell Protein Sox2 Confers Sensitivity to LSD1 Inhibition in Cancer Cells. *Cell Reports,* 5**,** 445-457.

ZHAO, H., SUN, Z. F., WANG, J., HUANG, H. J., KOCHER, J. P. & WANG, L. G. 2014. CrossMap: a versatile tool for coordinate conversion between genome assemblies. *Bioinformatics,* 30**,** 1006-1007.

ZHENG, Y., COHEN-KARNI, D., XU, D., CHIN, H. G., WILSON, G., PRADHAN, S. & ROBERTS, R. J. 2010. A unique family of Mrr-like modification-dependent restriction endonucleases. *Nucleic Acids Res,* 38**,** 5527-34.

ZHU, B., LIU, T., HU, X. & WANG, G. 2013. Developmental toxicity of 3,4-dichloroaniline on rare minnow (Gobiocypris rarus) embryos and larvae. *Chemosphere,* 90**,** 1132-9.

ZIBETTI, C., ADAMO, A., BINDA, C., FORNERIS, F., TOFFOLO, E., VERPELLI, C., GINELLI, E., MATTEVI, A., SALA, C. & BATTAGLIOLI, E. 2010. Alternative splicing of the histone demethylase LSD1/KDM1

904 contributes to the modulation of neurite morphogenesis in the mammalian nervous system. *J*
905 *Neurosci,* 30**,** 2521-32.

906

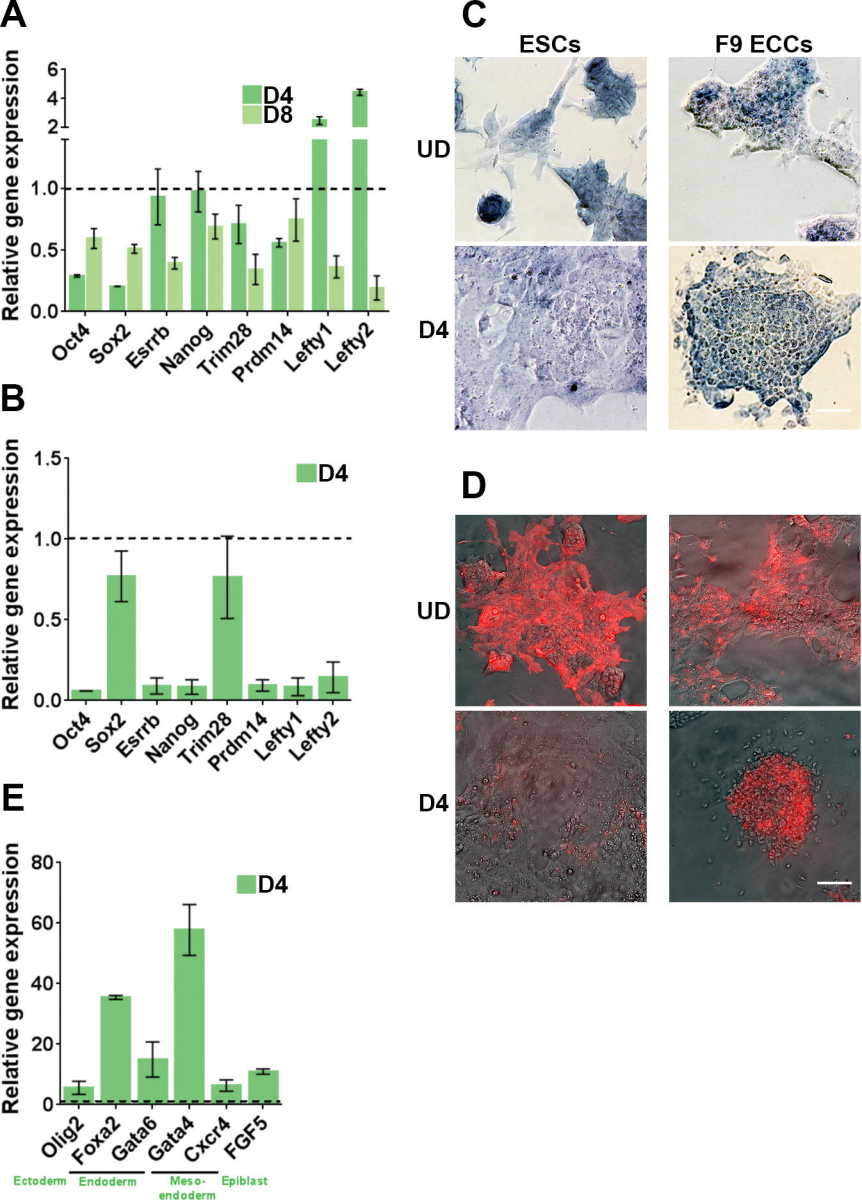
A
Relative gene expression
6
4
2
1.0
0.0
D4
D8
Oct4
Sox2
Esrrb
Nanog
Trim28
Prdm14
Lefty1
Lefty2
B
Relative gene expression
1.5
1.0
0.5
0.0
D4
Oct4
Sox2
Esrrb
Nanog
Trim28
Prdm14
Lefty1
Lefty2
C
ESCs
F9 ECCs
UD
D4
D
UD
D4
E
Relative gene expression
80
60
40
20
0
D4
Olig2
Foxa2
Gata6
Gata4
Cxcr4
FGF5
Ectoderm
Endoderm
Meso-endoderm
Epiblast

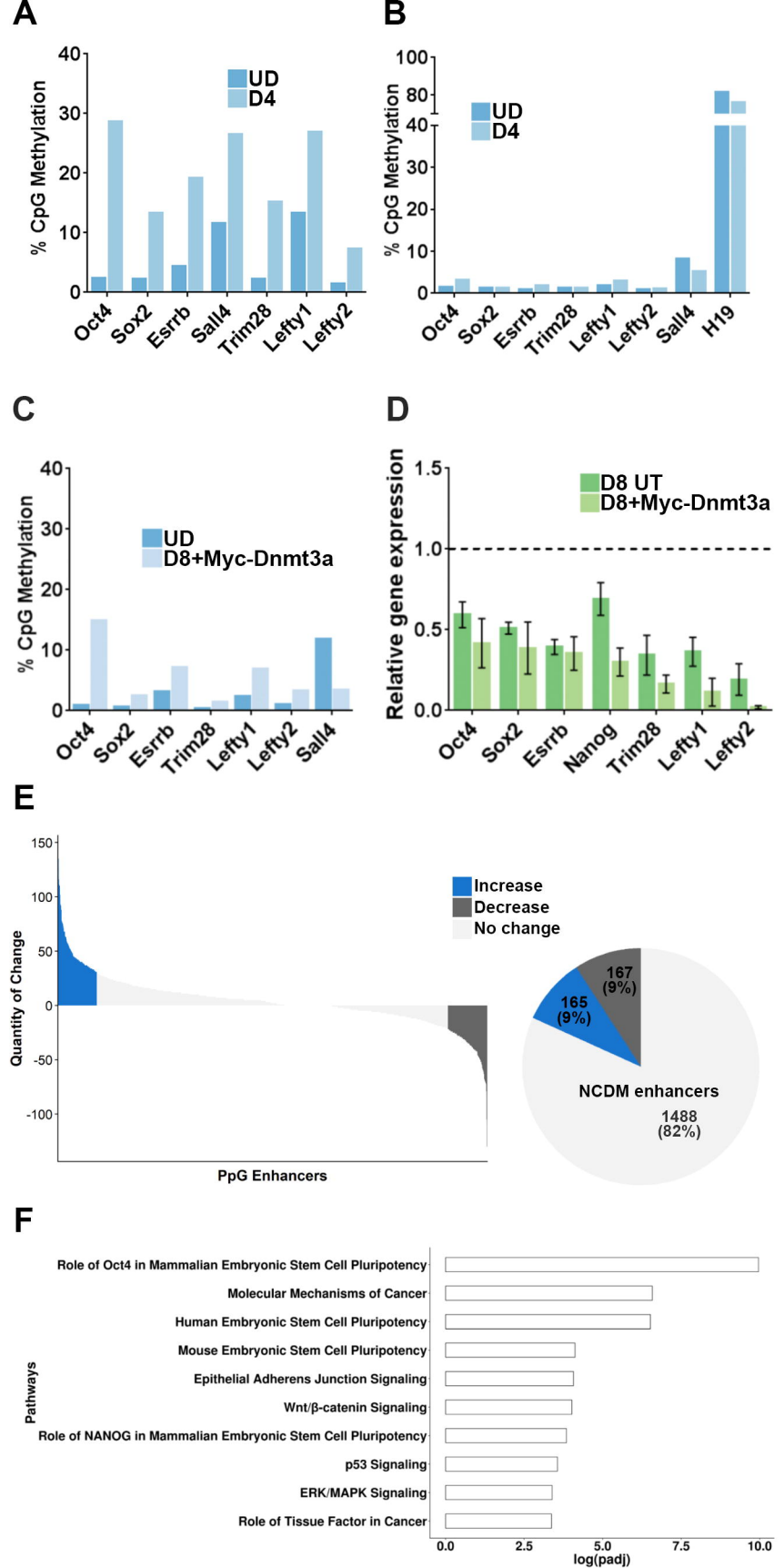
A
% CpG Methylation
UD
D4
Oct4
Sox2
Esrrb
Sall4
Trim28
Lefty1
Lefty2
B
% CpG Methylation
UD
D4
Oct4
Sox2
Esrrb
Trim28
Lefty1
Lefty2
Sall4
H19
C
% CpG Methylation
UD
D8+Myc-Dnmt3a
Oct4
Sox2
Esrrb
Trim28
Lefty1
Lefty2
Sall4
D
Relative gene expression
D8 UT
D8+Myc-Dnmt3a
Oct4
Sox2
Esrrb
Nanog
Trim28
Lefty1
Lefty2
E
Quantity of Change
PpG Enhancers
Increase
Decrease
No change
167
(9%)
165
(9%)
NCDM enhancers
1488
(82%)
F
Pathways
Role of Oct4 in Mammalian Embryonic Stem Cell Pluripotency
Molecular Mechanisms of Cancer
Human Embryonic Stem Cell Pluripotency
Mouse Embryonic Stem Cell Pluripotency
Epithelial Adherens Junction Signaling
Wnt/β-catenin Signaling
Role of NANOG in Mammalian Embryonic Stem Cell Pluripotency
p53 Signaling
ERK/MAPK Signaling
Role of Tissue Factor in Cancer
log(padj)

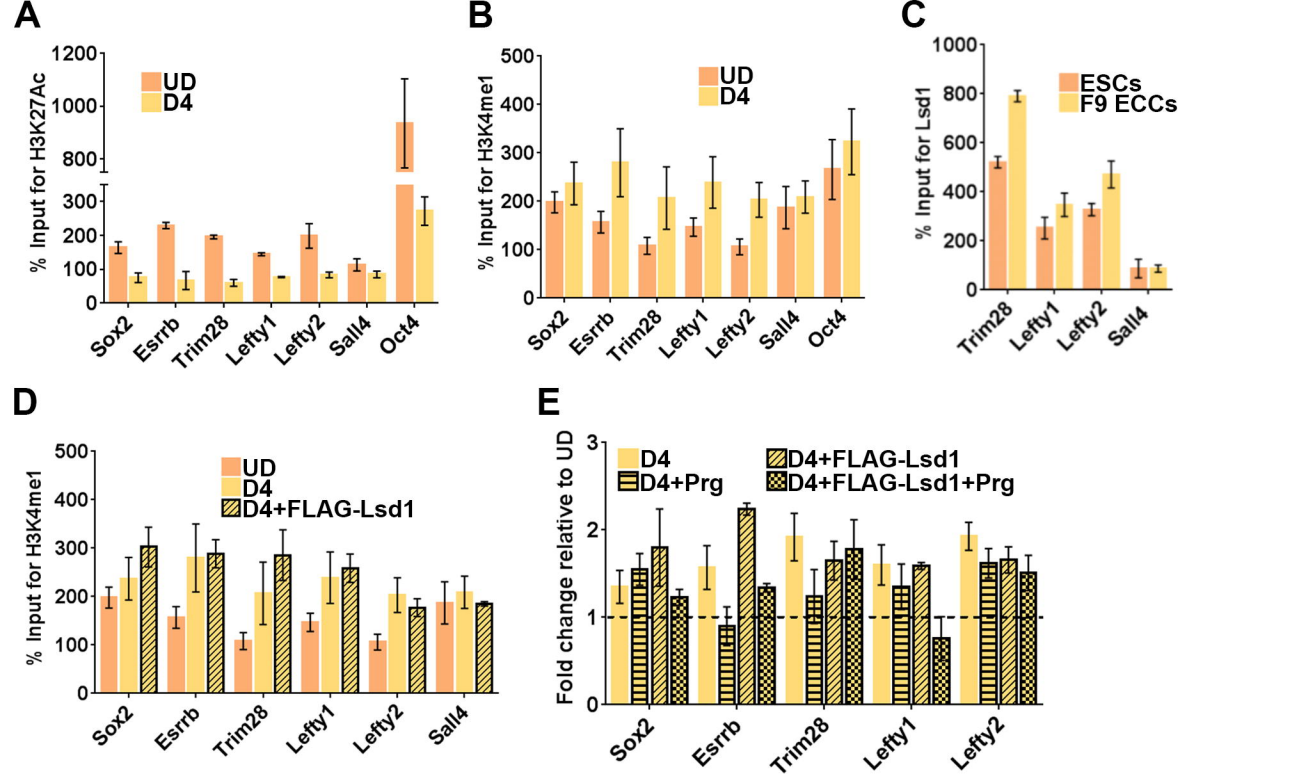
A
% Input for H3K27Ac
UD
D4
Sox2
Esrrb
Trim28
Lefty1
Lefty2
Sall4
Oct4
B
% Input for H3K4me1
UD
D4
C
% Input for Lsd1
ESCs
F9 ECCs
D
% Input for H3K4me1
UD
D4
D4+FLAG-Lsd1
E
Fold change relative to UD
D4
D4+Prg
D4+FLAG-Lsd1
D4+FLAG-Lsd1+Prg

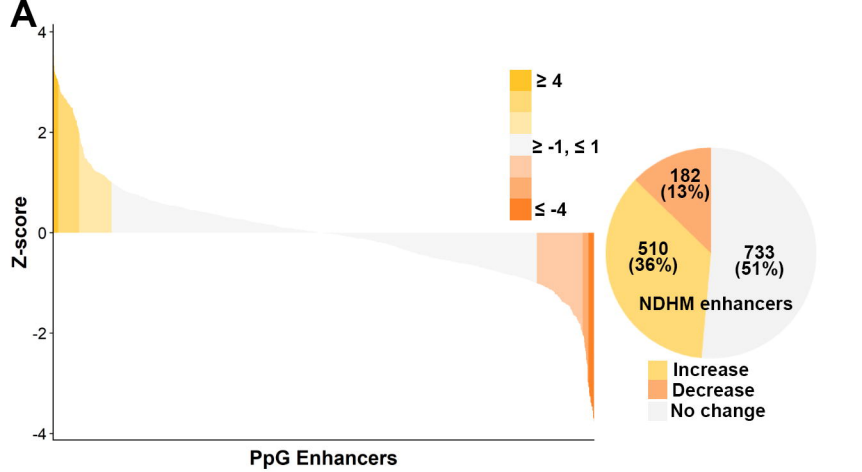
A
Z-score
4
2
0
-2
-4
PpG Enhancers
≥ 4
≥ -1, ≤ 1
≤ -4
182
(13%)
510
(36%)
733
(51%)
NDHM enhancers
Increase
Decrease
No change

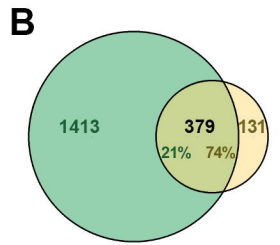
B
1413
379
131
21%
74%

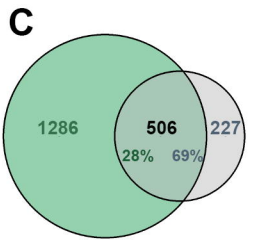
C
1286
506
227
28%
69%

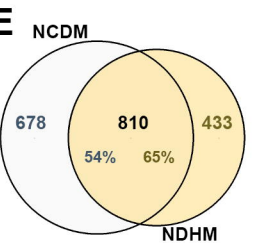
E
NCDM
678
810
433
54%
65%
NDHM

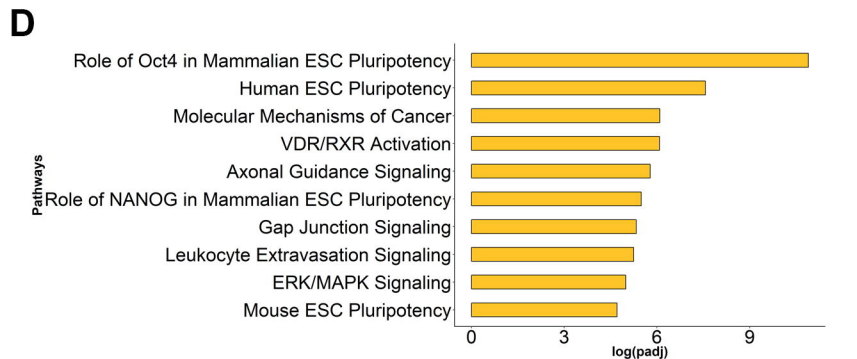
D
Role of Oct4 in Mammalian ESC Pluripotency
Human ESC Pluripotency
Molecular Mechanisms of Cancer
VDR/RXR Activation
Axonal Guidance Signaling
Role of NANOG in Mammalian ESC Pluripotency
Gap Junction Signaling
Leukocyte Extravasation Signaling
ERK/MAPK Signaling
Mouse ESC Pluripotency
Pathways
0
3
6
9
log(padj)

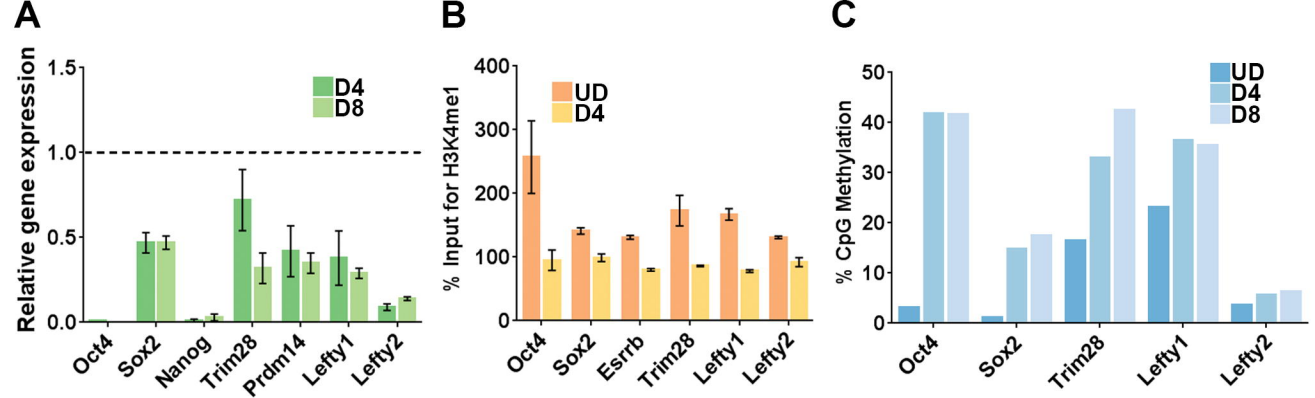
A
Relative gene expression
1.5
1.0
0.5
0.0
D4
D8
Oct4
Sox2
Nanog
Trim28
Prdm14
Lefty1
Lefty2
B
% Input for H3K4me1
400
300
200
100
UD
D4
Oct4
Sox2
Esrrb
Trim28
Lefty1
Lefty2
C
% CpG Methylation
50
40
30
20
10
0
UD
D4
D8
Oct4
Sox2
Trim28
Lefty1
Lefty2

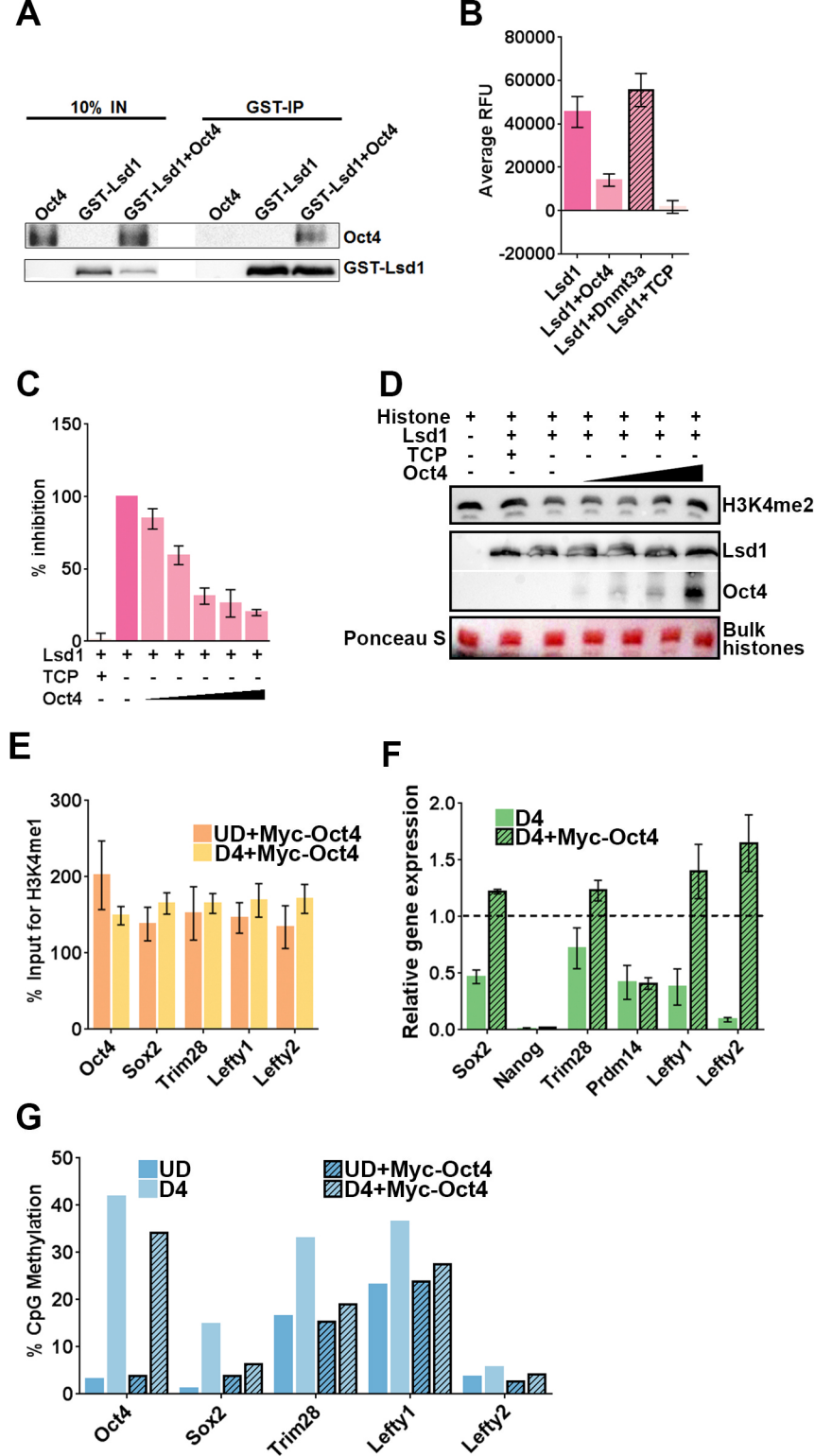
A
10% IN
GST-IP
Oct4
GST-Lsd1
GST-Lsd1+Oct4
Oct4
GST-Lsd1
GST-Lsd1+Oct4
Oct4
GST-Lsd1
B
Average RFU
80000
60000
40000
20000
0
-20000
Lsd1
Lsd1+Oct4
Lsd1+Dnmt3a
Lsd1+TCP
C
% inhibition
150
100
50
0
Lsd1
TCP
Oct4
D
Histone
Lsd1
TCP
Oct4
H3K4me2
Lsd1
Oct4
Ponceau S
Bulk histones
E
% Input for H3K4me1
300
200
100
0
UD+Myc-Oct4
D4+Myc-Oct4
Oct4
Sox2
Trim28
Lefty1
Lefty2
F
Relative gene expression
2.0
1.5
1.0
0.5
0.0
D4
D4+Myc-Oct4
Sox2
Nanog
Trim28
Prdm14
Lefty1
Lefty2
G
% CpG Methylation
50
40
30
20
10
0
UD
D4
UD+Myc-Oct4
D4+Myc-Oct4
Oct4
Sox2
Trim28
Lefty1
Lefty2

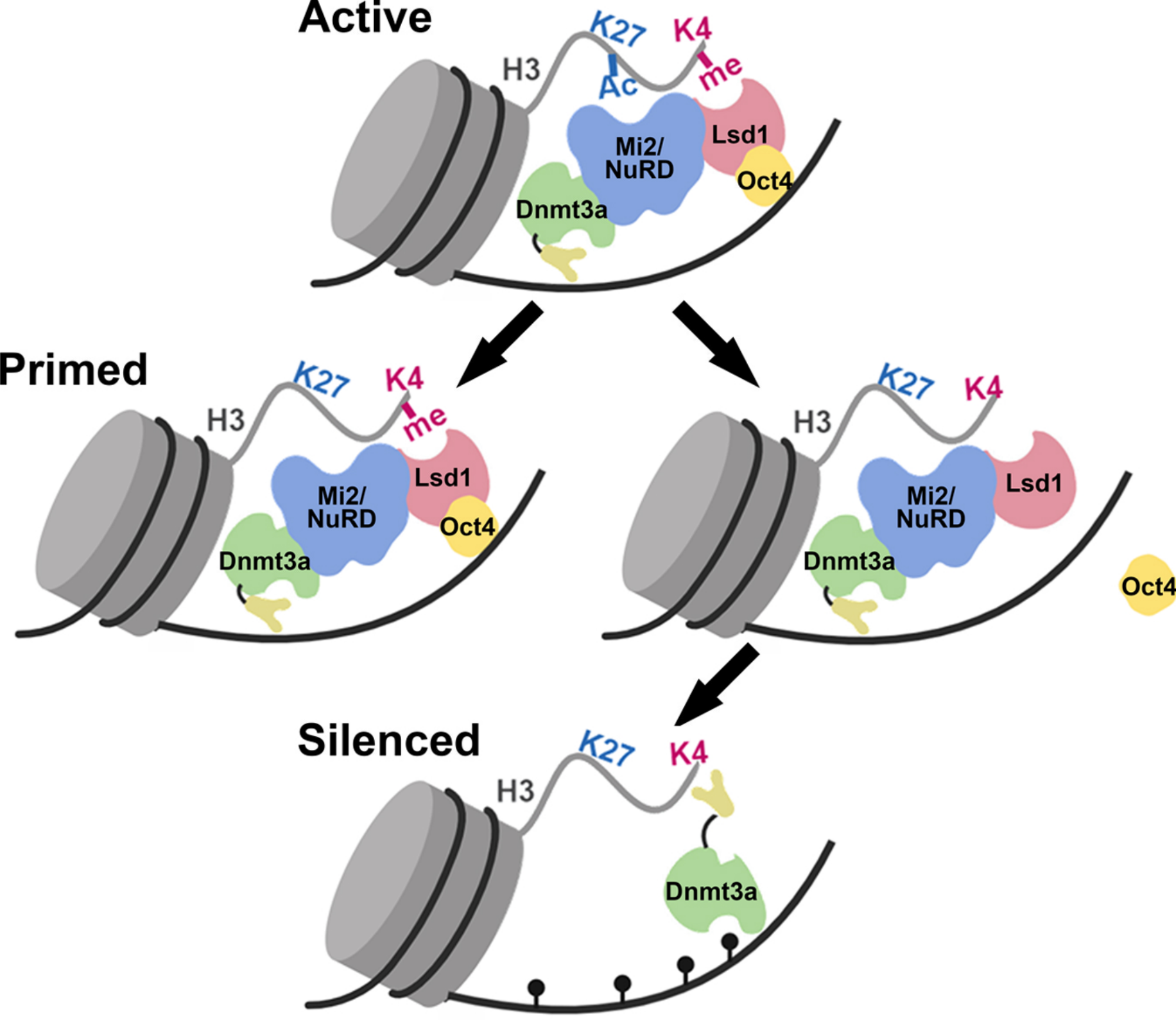
Active
H3
K27
K4
Ac
me
Mi2/
NuRD
Lsd1
Oct4
Dnmt3a
Primed
H3
K27
K4
me
Mi2/
NuRD
Lsd1
Oct4
Dnmt3a
H3
K27
K4
Mi2/
NuRD
Lsd1
Dnmt3a
Oct4
Silenced
H3
K27
K4
Dnmt3a